THE ANTARCTIC PALEOENVIRONMENT: A PERSPECTIVE ON GLOBAL CHANGE
ANTARCTIC RESEARCH SERIES, VOLUME 60, PAGES 1–25

SOUTHERN OCEAN INFLUENCES ON LATE EOCENE TO MIOCENE DEEPWATER CIRCULATION

JAMES D. WRIGHT

Lamont-Doherty Earth Observatory, Palisades, New York 10964

KENNETH G. MILLER[1]

Rutgers University, Department of Geological Sciences, Piscataway, New Jersey 08903

The Eocene through the Miocene marked the transition from warm polar climates of the early Eocene to the development of near-modern climates and deepwater patterns by the late Miocene. We reconstructed deepwater circulation patterns for the late Eocene through the Miocene using $\delta^{13}C$, $\delta^{18}O$, and sediment distribution. The $\delta^{13}C$ reconstructions and unconformities/hiatuses indicate that the Southern Ocean was the dominant deepwater source for the late Eocene through the Miocene with intervals of increased deepwater production at 40, 36, 30, and 15 Ma. Seismic stratigraphic and carbon isotopic evidence exists for a pulse of Northern Component Water (NCW) production during the earliest Oligocene, indicating that there was bipolar production of deep and bottom waters. Two additional intervals of enhanced NCW production followed in the Miocene, ~20 to 16 Ma and ~12 to 10 Ma. Each of the three intervals of NCW production correlates with an interval of erosion followed by drift development in the deep North Atlantic. Carbon isotope evidence for the production of warm saline deepwater (WSDW) in the mid-latitudes could be found only for the early Miocene, although $\delta^{18}O$ records indicate WSDW production during the late Eocene and early Oligocene.

INTRODUCTION

Warm salty water from the middle latitudes competes with cold, relatively fresh water from the high latitudes to fill the deep ocean basins. In today's ocean, high-latitude sources are dominant because the near-freezing polar conditions produce a denser in situ water mass than the mid-latitude evaporative regions. However, this may not have been true for ancient oceans. *Chamberlin* [1906] and *Brass et al.* [1982] postulated that warmer, saltier water from mid-latitude regions may have been the most dense water mass when polar regions were much warmer (e.g., the Cretaceous and early Eocene), thereby producing a warm deep-ocean circulation in contrast to today's cold deepwater regime.

Faunal, floral, and oxygen isotopic evidence shows that early Eocene high-latitude climates were unusually warm, making the early Eocene the most probable time during the Cenozoic for a dominance of middle latitude sources of warm saline deep water (WSDW) [e.g., *Haq*, 1981]. The warm high-latitude climates were associated with reduced meridional thermal gradients. *Shackleton and Boersma* [1981] estimated that Eocene sea surface temperature (SST) gradients from the low to high latitudes were approximately one half of the modern meridional gradient. Their planktonic foraminiferal $\delta^{18}O$ reconstruction highlighted two important differences between Eocene and modern surface waters: (1) Eocene equatorial SSTs may have been ~4°C cooler than at present, and (2) Eocene polar SSTs were 10°–15°C warmer than modern polar SSTs (Figure 1*a*). These estimates have become the cornerstone of modeling efforts that attempt to simulate unusually warm climates at high latitudes [e.g., *Barron*, 1983, 1987; *Manabe and Bryan*, 1985; *Rind*, 1987; *Covey and Barron*, 1988; *Covey and Thompson*, 1989; *Manabe et al.*, 1990; *Rind and Chandler*, 1991].

Paleotemperature estimates from foraminifera require estimates of the $\delta^{18}O_{water}$ in which the foraminifera lived. *Shackleton and Boersma* [1981] estimated Eocene SSTs using a uniform $\delta^{18}O_{water}$ value equal to the estimated global ocean $\delta^{18}O_{water}$ value. While these values are valid for the deepwater estimates, surface waters will have had different values because net evaporation enriches surface waters in ^{18}O in the low to middle latitudes and net precipitation depletes high-latitude surface waters with respect to ^{18}O. Modern surface water $\delta^{18}O_{water}$ values in tropical and subtropi-

[1]Also at Lamont-Doherty Earth Observatory, Palisades, New York, 10964.

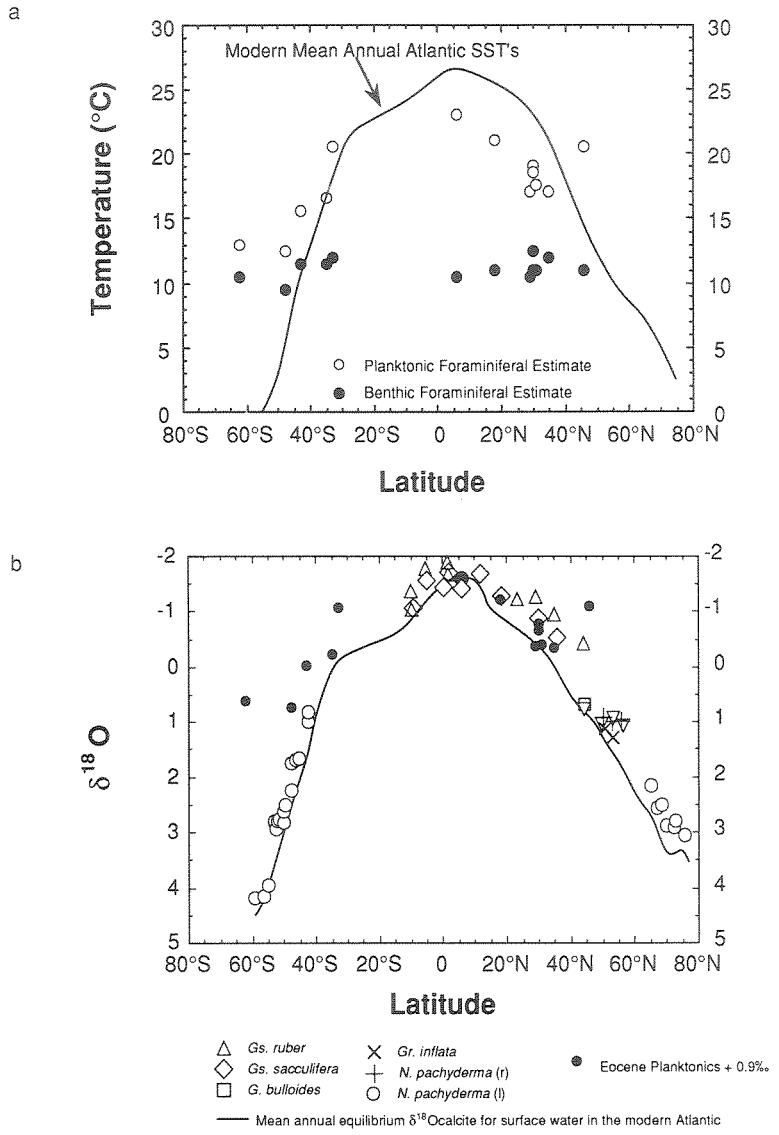

Fig. 1. (*a*) Estimated Eocene surface and deepwater temperatures from planktonic and benthic foraminiferal $\delta^{18}O$ values [*Shackleton and Boersma*, 1981] relative to the modern mean annual SSTs for the Atlantic Ocean. *Shackleton and Boersma* [1981] used a mean ocean $\delta^{18}O$ of seawater difference of ~0.9‰ between the modern ocean and an ice-free Eocene in their paleotemperature equation. (*b*) Comparison of the modern planktonic $\delta^{18}O$ profile in the Atlantic (R. G. Fairbanks et al., work in preparation) with the Eocene values from *Shackleton and Boersma* [1981]. We added a constant value of 0.9‰ to the Eocene values [*Shackleton and Kennett*, 1975] to account for the difference between mean ocean $\delta^{18}O$ values during the ice-free Eocene and the present. The Eocene $\delta^{18}O$ gradient is remarkably similar to the modern gradient from 40°N to 40°S. The observation of cooler Eocene tropical temperatures is not supported by this comparison. However, the middle to high latitudes were remarkably different showing a >3‰ difference at 60°S.

cal regions are higher than the mean ocean value by approximately 1‰ [*Craig and Gordon*, 1965]. This difference suggests that Shackleton and Boersma's equatorial estimates may not be correct. A paleotemperature estimate without consideration of $\delta^{18}O_{water}$ variations due to evaporation will produce cooler temperature estimates, and therefore the Eocene SST estimates may have been as much as 4°C too cold. To avoid this problem, we compared *Shackleton and Boersma*'s [1981] Eocene planktonic foraminiferal $\delta^{18}O$ profile with a modern Atlantic profile (R. G. Fairbanks et al., work in preparation). Both profiles are similar for the low- to mid-latitude regions when ice volume differences between an ice-free Eocene and modern ice volume are taken into account (Figure 1*b*) (R. G. Fairbanks et al., work in preparation). This comparison suggests that Eocene equatorial SSTs may have been closer to the modern average of 28°C than the 24°C estimated by

Shackleton and Boersma [1981], although more detailed reconstructions show cooler tropical SSTs for certain intervals during the Eocene [*Zachos et al.*, 1993]. With regard to the high-latitudes SSTs, Shackleton and Boersma's comparison (Figure 1) shows that polar surface waters were 10°–15°C warmer during the early Eocene than at present (Figure 1), which is consistent with the conclusions of other studies [e.g., *Shackleton and Kennett*, 1975; *Savin et al.*, 1975; *Shackleton and Boersma*, 1981; *Kennett and Stott*, 1990; *Stott et al.*, 1990; *Barrera and Huber*, 1991; *Zachos et al.*, 1993].

Sea surface temperatures play a direct role in modulating deepwater formation and, hence, govern deepwater temperatures. Polar SST fluctuations are transmitted directly to the deep ocean during intervals when deep water is formed predominantly in polar regions. However, if polar SSTs warm substantially, then the deep waters may acquire properties derived from mid-latitude sources. This may have been the case for the early Eocene [*Kennett and Stott*, 1990; *Pak and Miller*, 1992], when deepwater temperatures were warmest, reaching temperatures of 10°–14°C (*Shackleton and Kennett* [1975], *Savin et al.* [1975], and *Miller et al.* [1987]; Figure 1). From this maximum, both deep and polar surface water temperatures cooled by ~9°C to 2°–4°C by the early Oligocene [*Shackleton and Kennett*, 1975; *Savin et al.*, 1975; *Miller et al.*, 1987; *Miller*, 1992]. This cooling was recorded in benthic and high-latitude planktonic foraminiferal $\delta^{18}O$ values, which increased by ~3.0‰ during this interval with a final increase of ~1.0‰ at the Eocene/Oligocene boundary (Figure 2).

Kennett and Shackleton [1976] proposed that a 1.0‰ $\delta^{18}O$ increase in the benthic foraminifera near the Eocene/Oligocene boundary represented the development of psychrospheric conditions or ventilation of the deep ocean by cold deepwater masses (i.e., thermohaline conditions similar to the present). Another important development was the discovery by *Kennett and Stott* [1990] that late Eocene and early Oligocene benthic foraminiferal $\delta^{18}O$ values on Maud Rise were inverted in relation to modern gradients; high values occurred at intermediate depths (~1500 m), while lower values occurred at greater depths (~2200 m) (Figure 2). Largely on the basis of these $\delta^{18}O$ records, *Kennett and Stott* [1990] proposed that there were three general stages of Cenozoic deepwater circulation:

1. Eocene and possibly Paleocene deepwater circulation was driven by halothermal processes or deepwater convection based largely on salinity-induced density differences. This halothermal circulation was designated the Proteus Ocean, and it consisted of warm saline deepwater overlain by a colder, fresher water mass. WSDW originated in low-latitude regions (Tethyan) where evaporation exceeded precipitation and runoff, creating the densest water mass. A colder, fresher water mass originated in the Southern Ocean, but it penetrated only to intermediate depths because of its lower salinity.

2. Oligocene deepwater circulation (Proto-Oceanus) represented the transition between the halothermal Proteus and thermohaline Oceanus (Neogene). This ocean consisted of three components; two cold, relatively fresh water masses that originated in the high southern latitudes which were separated by a warm saline layer. The deepest water mass was analogous to Antarctic Bottom Water (AABW) and may have been aided by the formation of sea ice around Antarctica.

3. The Neogene deep oceans were ventilated by the thermohaline circulation that resulted from freezing conditions in the high latitudes. There was little deepwater (i.e., below 2 km) ventilation by WSDW production in this psychrospheric ocean designated as Oceanus.

The *Kennett and Stott* [1990] scenario has stimulated much discussion in the paleoceanographic community. In addition to the stable isotopic data from Maud Rise, there is evidence from sediment distributions that broadly supports many of their conclusions. For example, lower and middle Eocene unconformities are rare [*Moore et al.*, 1978], and the conformable nature of seismic reflectors indicates that deepwater circulation was generally sluggish during the early and middle Eocene and possibly in the late Eocene [*Tucholke and Mountain*, 1979, 1986; *Miller and Tucholke*, 1983; *Mountain and Miller*, 1992]. Such a sluggish circulation is consistent with low-temperature gradients with respect to latitude and depth. These lower-temperature gradients would result in low-density gradients and low ocean turnover times relative to the colder intervals which followed. In addition, the calcite compensation depth (CCD) was relatively shallow during the Eocene [*van Andel*, 1975], and the surface to deep $\delta^{13}C$ differences were unusually large [*Boersma et al.*, 1987], which are consistent with slow ventilation of the deep oceans during the Eocene and/or unusually high mean ocean nutrient levels. This period of relative quiescence during the early and middle Eocene ended with an interval of more vigorous deepwater production in the Southern Ocean and the North Atlantic that caused widespread erosion during the late Eocene and earliest Oligocene [*Kennett*, 1977; *Miller and Tucholke*, 1983].

We review the evidence for late Eocene to Miocene deepwater circulation changes in view of the *Kennett and Stott* [1990] hypothesis, focusing on oxygen and carbon isotopic records and sediment distribution. We relate deepwater circulation changes to tectonic and global climate reorganizations that occurred from the late Eocene to the Miocene. This interval is critical to our understanding of climate change because (1) it represents the transition from the warm Eocene climates to the northern hemisphere glacial/interglacial cycles in the Pliocene, (2) it contains the first definitive evidence for Antarctic ice sheet growth, and (3) it

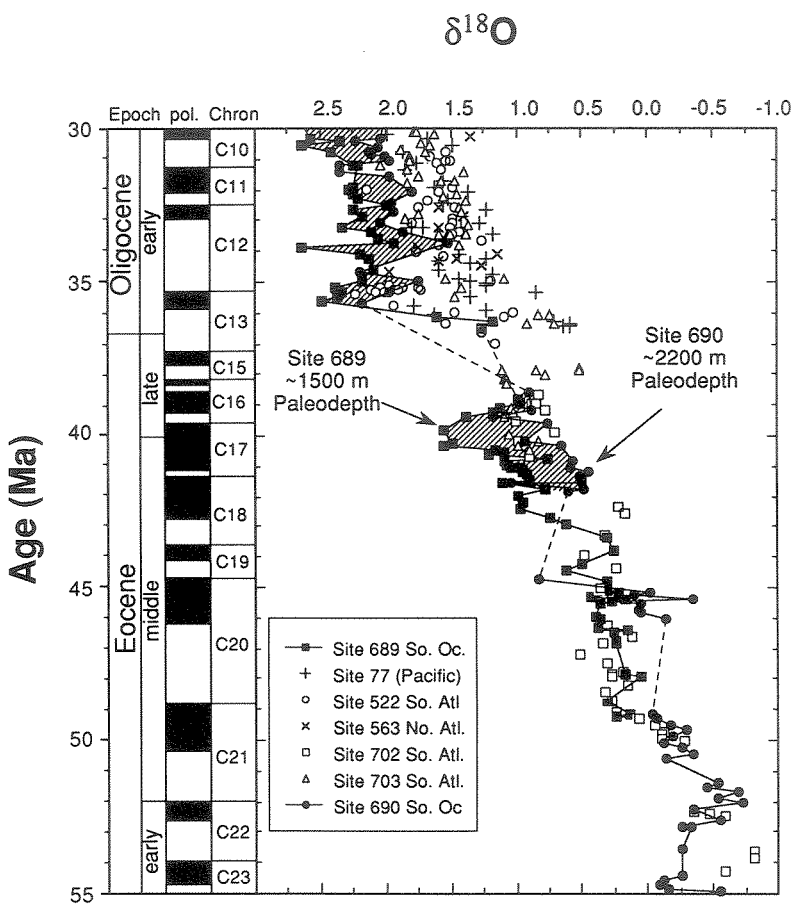

Fig. 2. Late Paleocene to early Oligocene *Cibicidoides* $\delta^{18}O$ records for Ocean Drilling Program (ODP) sites 689 and 690 on Maud Rise [*Kennett and Stott*, 1990] compared to *Cibicidoides* $\delta^{18}O$ records from other regions (Site 77 [*Keigwin and Keller*, 1984], Site 522 [*Miller et al.*, 1988], Site 563 [*Miller and Fairbanks*, 1985], Site 702 [*Katz and Miller*, 1992], and Site 703 [*Miller*, 1992]). Late Eocene to early Oligocene paleodepths for sites 689 and 690 are estimated to have been ~1500 m and ~2200 m, respectively. The hachured areas highlight two intervals when the deeper site on Maud Rise (Site 690) recorded lower $\delta^{18}O$ values by 0.5 to 1.0‰. Because temperature dominates the $\delta^{18}O_{calcite}$ in the modern ocean, deep-ocean *Cibicidoides* $\delta^{18}O$ values are expected to increase with depth. However, warmer, but more salty water may become more dense during warm climate intervals. Therefore *Kennett and Stott* [1990] interpreted this "$\delta^{18}O$ inversion" as reflecting a warm saline deepwater mass. It is important to note that the deeper site (Site 690) recorded values more similar to mean deepwater conditions than the site at intermediate depths (Site 689).

represents a fundamental change in deepwater circulation from a warm to a cold system.

DEEPWATER CIRCULATION PATTERNS

Carbon Isotope Reconstructions

Carbon isotopes provide a powerful tracer for reconstruction of deepwater circulation patterns. The GEOSECS transects are the foundation for using $\delta^{13}C$ distributions to record changes in deepwater circulation. *Kroopnick* [1985] documented that the distribution of $\delta^{13}C$ in oceanic dissolved bicarbonate accurately reflects modern deepwater circulation patterns (Figure 3). Two processes modify deepwater $\delta^{13}C$ values once a water mass is isolated from the surface ocean and the atmosphere: (1) mixing with a water mass of different isotopic composition and (2) the accumulation of oxidized organic matter, commonly referred to as "deepwater aging." In the modern Atlantic Ocean, $\delta^{13}C$ changes predominantly reflect mixing between North Atlantic Deep Water (NADW) with high $\delta^{13}C$ values (1.0‰) and Southern Component Water (SCW) with lower $\delta^{13}C$ values (0.4‰) (Figure 3). The residence time of deep water within the Atlantic is short (<350 years), and overlying surface productivity is low, thereby limiting any significant accumulation of oxidized organic

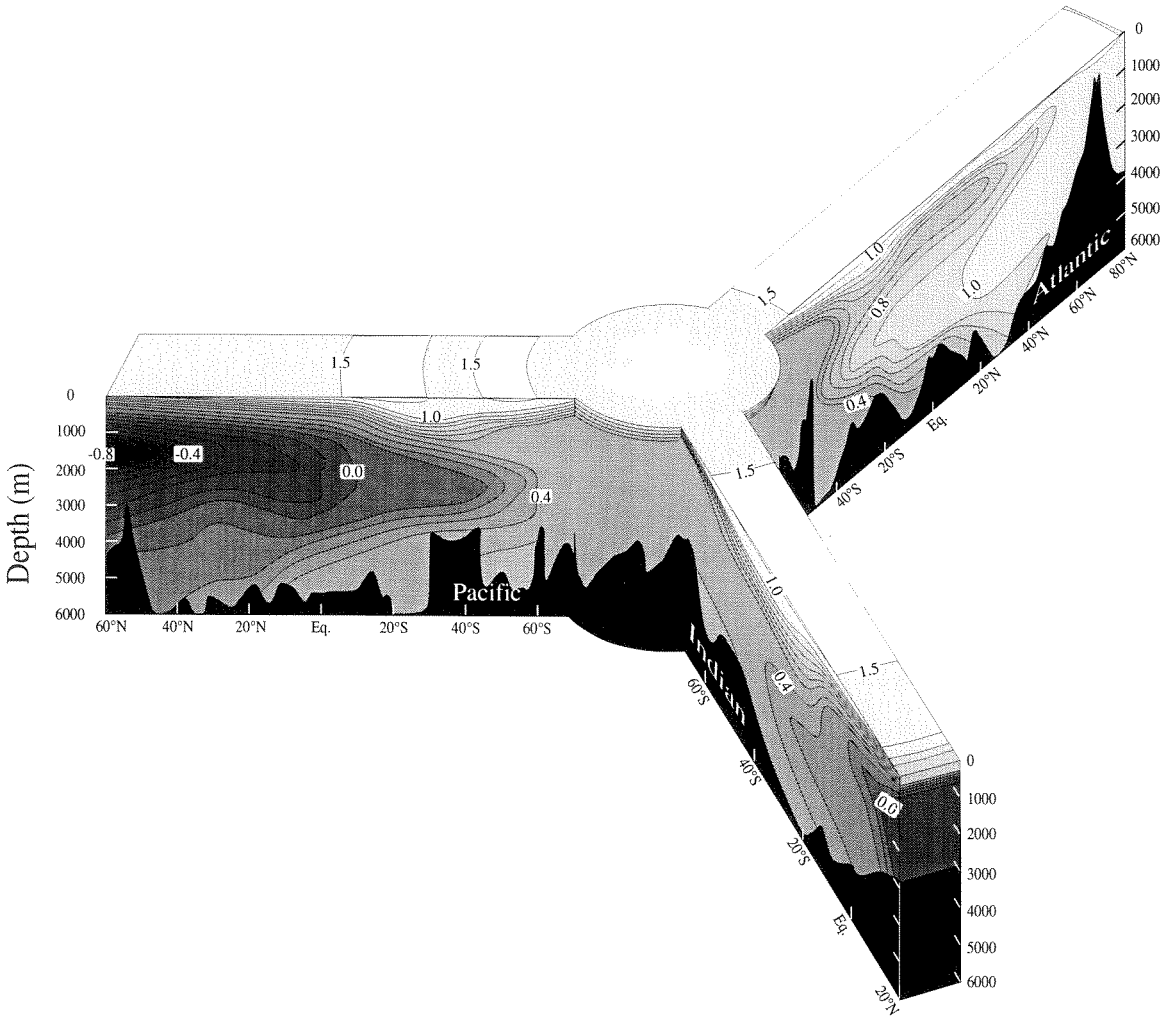

Fig. 3. The distribution of $\delta^{13}C$ in the world's ocean is a reflection of modern deepwater circulation patterns (adapted from *Kroopnick* [1985]). Pacific Ocean $\delta^{13}C$ values approximate the mean ocean water $\delta^{13}C$ value because of its large volume. Deep Atlantic $\delta^{13}C$ values are higher than those in the Pacific because the deep water ventilating the Atlantic, North Atlantic Deep Water (NADW), has a large surface water component. Surface waters are enriched in ^{13}C owing to biological activity which preferentially removes ^{12}C from the surface water. The Southern Ocean $\delta^{13}C$ value is dependent on the deepwater contribution from the Atlantic, Indian, and Pacific oceans [*Oppo and Fairbanks*, 1987]. At present the Southern Ocean is higher than the Pacific because of a high NADW flux. During the last glacial maximum, Pacific Ocean and Southern Ocean $\delta^{13}C$ values were much closer to each other because of the reduced NADW influence [*Oppo and Fairbanks*, 1987; *Charles and Fairbanks*, 1992].

matter within these basins [*Broecker*, 1979]. Conversely, Pacific Ocean and Indian Ocean $\delta^{13}C$ changes result from deepwater aging (Figure 3). Both oceans are ventilated from south to north by one deepwater mass, Southern Component Water. In the Pacific and Indian oceans, longer deepwater residence times (>1000 years for the Pacific [*Broecker et al.*, 1988; *Broecker*, 1989]), relatively high surface water productivity in the equatorial regions, and the lack of a northern deepwater counterpart produce a south to north $\delta^{13}C$ gradient due to aging (Figure 3). In general, locations proximal to deepwater sources will record higher $\delta^{13}C$ values than more distal sites.

We have a paleorecord of these processes because certain benthic foraminiferal genera (*Cibicidoides and Planulina*) accurately record the $\delta^{13}C$ gradients of the deepwater masses [*Shackleton and Opdyke*, 1973; *Duplessy et al.*, 1970; *Belanger et al.*, 1981; *Graham et al.*, 1981]. Carbon isotope studies have provided detailed reconstructions of Pleistocene deepwater changes using

both time series and time slice approaches [e.g., *Shackleton et al.*, 1983; *Boyle and Keigwin*, 1982, 1987; *Curry and Lohmann*, 1982; *Oppo and Fairbanks*, 1987; *Curry et al.*, 1988; *Duplessy et al.*, 1988; *Oppo et al.*, 1990]. We employ similar strategies for Eocene-Miocene reconstructions, using both time series and time slices. The time series approach requires relatively complete records from strategic locations and provides a chronology of deepwater circulation changes [e.g., *Oppo and Fairbanks*, 1987]. It is also necessary to use time slice reconstructions to determine the three-dimensional aspect of circulation changes (e.g., *Duplessy et al.* [1988] for the last glacial maximum and *Woodruff and Savin* [1989] and *Wright et al.* [1992] for the Miocene). The combination of both approaches provides a comprehensive evaluation of deepwater circulation patterns.

Late Eocene to Oligocene $\delta^{13}C$ reconstructions. The largest basin to basin $\delta^{13}C$ differences during the late Eocene to Oligocene were 0.5‰, which is one half of the modern difference (Atlantic-Pacific $\Delta\delta^{13}C$ is currently 1.0‰ (Figure 4)) [*Miller and Fairbanks*, 1985; *Boersma et al.*, 1987]. The low $\delta^{13}C$ differences can reflect (1) lower mean ocean nutrient levels during this interval relative to modern levels [*Boyle*, 1988], (2) a one-component deepwater circulation system, although this requires high ventilation rates in order to minimize aging effects, or (3) multiple sources with similar $\delta^{13}C$ values. While the oligotrophic nature and inferred low nutrients of the Oligocene oceans have been noted [e.g., *Miller and Fairbanks*, 1985; *Boersma et al.*, 1987], better quantification with nutrient proxies (such as Cd/Ca ratios in benthic foraminifera) is needed to substantiate this observation. Lower mean ocean nutrients during the late Eocene through the Oligocene may account for much of the low basin-basin $\delta^{13}C$ difference as also evidenced by low vertical (surface to deep) $\delta^{13}C$ gradients [*Miller and Fairbanks*, 1985; *Boersma et al.*, 1987]. Although the decreased sensitivity (dynamic range) of $\delta^{13}C$ as a tracer results from lower mean ocean nutrients, $\delta^{13}C$ reconstructions still provide information on deepwater circulation changes.

There are few suitable upper Eocene sections available for detailed stable isotopic studies; therefore our interpretation of deepwater circulation patterns based on $\delta^{13}C$ reconstructions is inconclusive for this interval. Available late Eocene $\delta^{13}C$ records show similar values in the major ocean basins, making it difficult to identify a deepwater source region (Figure 4). A three-dimensional representation of the late Eocene $\delta^{13}C$ patterns also shows that values were similar in all the major ocean basins (Figure 5). However, there is an intriguing hint of a deep to intermediate water source originating outside of the Southern Ocean during this interval. Carbon isotope values from Site 549 in the eastern North Atlantic were higher than those in the Southern Ocean from the late middle to early late Eocene (~41 to 38 Ma; Figure 4). (We use the geomagnetic polarity time scale (GPTS) of *Berggren et al.* [1985] throughout. Large changes in the Paleogene portions of the GPTS have been proposed [*Cande and Kent*, 1992], with some epoch boundaries changing by more than 2 m.y. Although this change will affect the absolute chronology of the events discussed herein, it will not alter their relative chronologies.) Although more data are needed from Site 549 to establish this difference, it implies that this region was proximal to a deep to intermediate source (late Eocene paleodepth estimates for Site 549 are ~2000 m [*Miller et al.*, 1985]). As a result, we can only infer that the high $\delta^{13}C$ values at Site 549 represent either a source of Northern Component Water (NCW) or western outflow of Tethyan water, but not the depth to which this water penetrated. The present core coverage is inadequate to distinguish between the two.

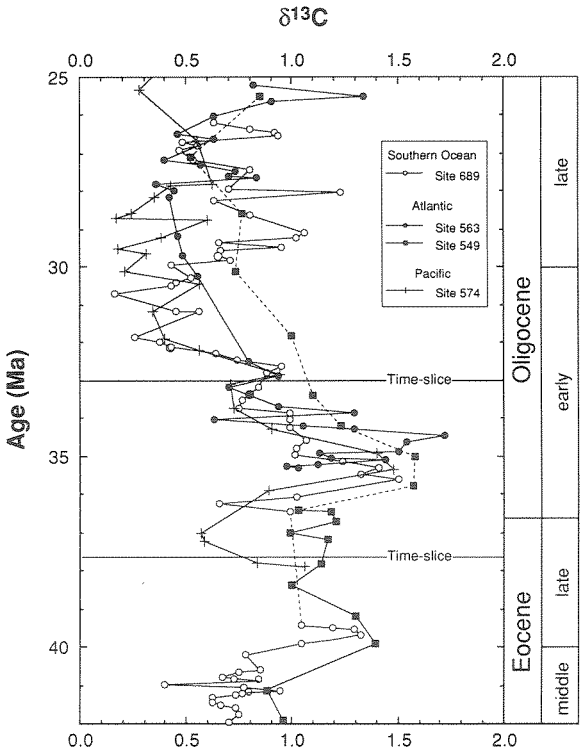

Fig. 4. Late Eocene to Oligocene $\delta^{13}C$ records from the Southern, Atlantic, and equatorial Pacific oceans (Site 689 [*Kennett and Stott*, 1990], Site 574 [*Miller and Thomas*, 1985], Site 563 [*Miller and Fairbanks*, 1985], and Site 549 [*Miller et al.*, 1985]). Basin to basin $\delta^{13}C$ differences were small (≤0.5‰) throughout this interval relative to the modern basin to basin differences (1.0). North Atlantic Site 549 (~2000-m paleodepth) recorded high $\delta^{13}C$ values relative to the Southern Ocean during the late Eocene to Oligocene, indicating its proximity to an intermediate water or deepwater source. This source may have been WSDW flowing out of the western Tethys or an upper limb of NCW. Time slice reconstructions shown in Figures 5 and 7 are marked.

The Oligocene was dominated by Southern Compo-

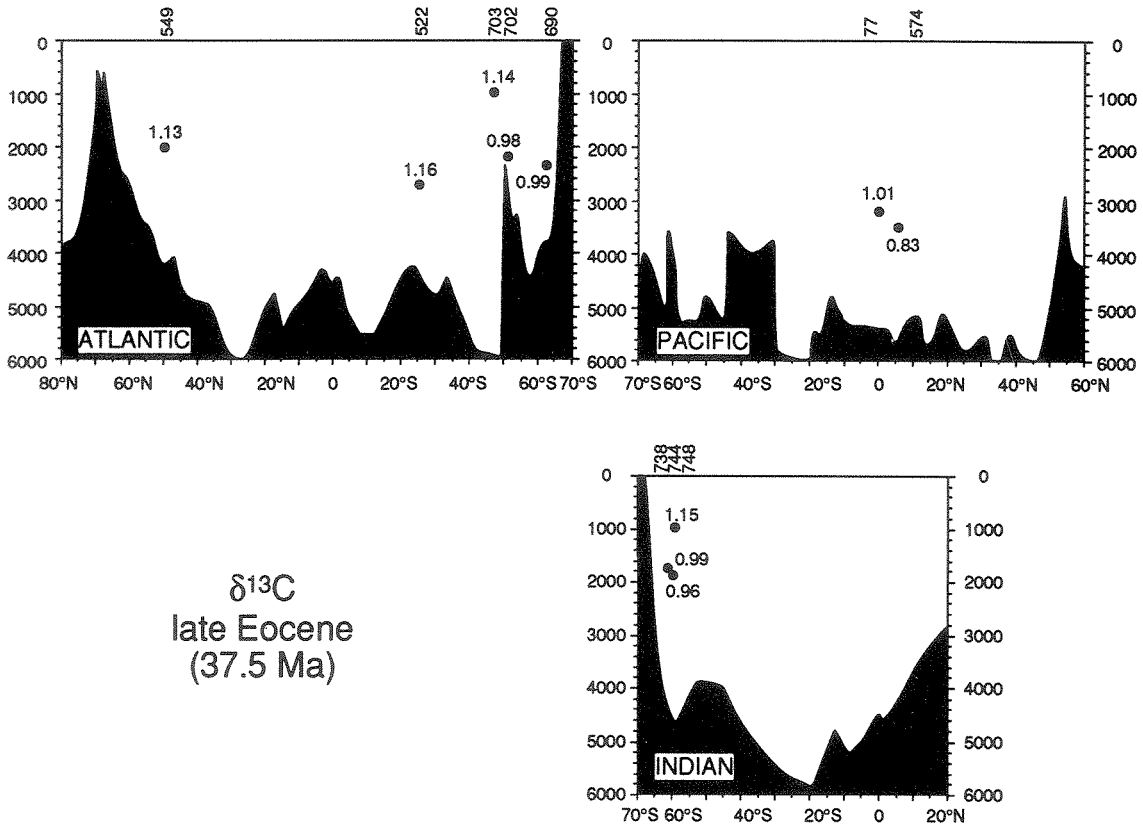

Fig. 5. Late Eocene $\delta^{13}C$ cross section of the oceans at 37.5 Ma. There is very little gradient (0.2‰) among the deepwater sites in all three oceans. The highest values were consistently recorded at intermediate depths as well as in the North Atlantic. This is consistent with an intermediate water mass which originated outside of the Southern Ocean. Two probable sources were either WSDW from the Tethys or an upper limb of NCW. Stratigraphic levels and data sources for each site are listed in Table 1*a*.

nent Water (analogous to AABW [*Broecker and Peng*, 1982]). Although the basin to basin $\delta^{13}C$ differences during the Oligocene remained low, it is evident that the Southern Ocean $\delta^{13}C$ values were equal to or higher than those recorded at other deepwater sites (e.g., sites 563 and 77; Figure 4). *Miller* [1992] noted a brief exception to this during the earliest Oligocene. From ~35.5 to 34.5 Ma, the highest deepwater $\delta^{13}C$ values were recorded in the North Atlantic, lowest values were recorded in the Pacific, and intermediate values were recorded in the Southern Ocean (Figure 6). This pattern is similar to the modern distribution of $\delta^{13}C$ values that reflect the production of both NCW and SCW. This is the first documented interval of bipolar deepwater production during the Cenozoic [*Miller*, 1992]. It is unlikely that the observed offsets are an artifact of a miscorrelation of the North Atlantic Site 563 record because the age estimates were based on magnetostratigraphic and $\delta^{18}O$ correlations. For the remainder of the Oligocene, the $\delta^{13}C$ patterns indicate a return to a one-component deepwater system that can be traced to the Southern Ocean (Figures 4 and 6). Oligocene oxygen isotope comparisons are consistent either with a single source with intermediate depth, Site 689, reflecting the "cold spigot" being diluted by mean ocean water (Figure 2) [*Miller*, 1992; this study], or with two sources, WSDW and Southern Ocean [e.g., *Kennett and Stott*, 1990] (see below for discussion).

The uniformity of early Oligocene $\delta^{13}C$ values is illustrated in the 33 Ma time slice (Figure 7). Core coverage is best in the Atlantic Ocean and shows little variation (~0.2‰) at sites with paleodepths greater than 2000 m. With the exception of Site 549, which apparently was influenced by an intermediate to upper deepwater mass of unknown origin, South Atlantic $\delta^{13}C$ values were similar to or slightly higher than those in the North Atlantic, which is consistent with a south to north deepwater flow. Two deep Pacific sites recorded values similar to those in the Atlantic and Southern oceans (Figure 7). As was noted previously, near-uniform Oligocene deep-ocean $\delta^{13}C$ values probably resulted from relatively low mean ocean nutrients combined with a

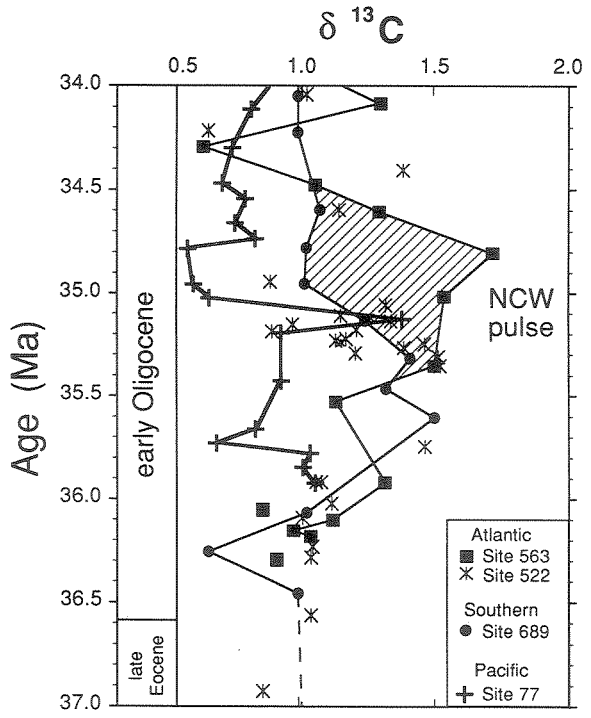

Fig. 6. Earliest Oligocene benthic foraminiferal $\delta^{13}C$ records from the North Atlantic (Site 563, solid squares), Southern Ocean (Site 689, solid circles), and Pacific (Site 77, crosses) oceans. From 36.2 to 35.5 Ma, the North Atlantic and Southern oceans recorded similar $\delta^{13}C$ values, reflecting SCW filling the North Atlantic. Beginning at 35.5 Ma and continuing through 34.5 Ma, the North Atlantic recorded the highest $\delta^{13}C$ values, Southern Ocean values were intermediate values, and the Pacific values were the lowest. This pattern is the same $\delta^{13}C$ pattern observed in the modern ocean. This interval from 35.5 to 34.5 Ma is interpreted as the first record of bipolar production of deep water during the Cenozoic [*Miller*, 1992].

dominant Southern Ocean deepwater source. To maintain similar $\delta^{13}C$ values with one source requires high ventilation rates; otherwise, aging effects would be more apparent. High ventilation rates for the Oligocene are consistent with a dramatic lowering of the CCD [*van Andel*, 1975] at this time.

Miocene $\delta^{13}C$ reconstructions. A consensus has developed concerning the middle and late Miocene deepwater circulation history; however, early Miocene deepwater circulation patterns remain controversial. *Woodruff and Savin* [1989] and *Wright et al.* [1992] compiled two comprehensive syntheses of Miocene deepwater circulation patterns. In general, both studies found that the major deepwater changes followed the subdivisions of this epoch. Early Miocene deepwater circulation patterns consisted of as many as three independent water masses, two of which were relatively warm and salty (Tethyan water [*Woodruff and Savin*, 1989] and NCW [*Wright et al.*, 1992]). Production of these warm deepwater sources diminished during the middle Miocene before a pattern much like today's developed during the late Miocene.

Almost all studies of Miocene deepwater circulation patterns have concluded that NCW (re)developed during the middle Miocene and reached near-modern fluxes during the late Miocene [*Blanc et al.*, 1980; *Schnitker*, 1980; *Bender and Graham*, 1981; *Woodruff and Savin*, 1989; *Wright et al.*, 1991, 1992]. *Vogt* [1972] was the first to propose that subsidence of the Greenland-Scotland Ridge was responsible for NCW production in an effort to explain evidence for intensified bottom water currents in the North Atlantic between 18 and 10 Ma [*Ruddiman*, 1972]. Two subsequent studies built on this idea. *Blanc et al.* [1980] and *Schnitker* [1980] independently proposed that North Atlantic salinities increased in the middle Miocene as the eastern Tethys closed, shunting warm salty water into the North Atlantic; together with subsidence of the Greenland-Scotland Ridge, this contributed to NCW formation. *Woodruff and Savin* [1989] provided the first comprehensive global synthesis of Miocene benthic foraminiferal isotope data. In regard to global deepwater circulation patterns, *Woodruff and Savin* [1989] concluded that (1) SCW was the dominant water mass ventilating the deep oceans during the Miocene, (2) a warm saline plume originated in the Tethys and was an important component of deepwater circulation and climate during the early Miocene, (3) there is little evidence for NCW prior to 12–10 Ma, and (4) late Miocene deepwater circulation patterns were similar to the modern patterns. Their $\delta^{13}C$ results were consistent with those of *Blanc et al.* [1980] and *Schnitker* [1980], indicating that a NCW flux developed during the middle Miocene. The most striking feature of the *Woodruff and Savin* [1989] time slices was a high $\delta^{13}C$ water mass in the Indian Ocean during much of the early Miocene. They interpreted this signal as WSDW that originated in the Tethys.

In contrast to these studies, *Miller and Fairbanks* [1983, 1985] suggested that NCW was produced as early as the Oligocene. They noted that North Atlantic $\delta^{13}C$ values were higher than those in the Pacific during much of the Miocene, arguing for the presence of NCW during this interval. *Wright et al.* [1992] combined time series and time slice $\delta^{13}C$ reconstructions in an attempt to resolve discrepancies concerning early and middle Miocene deepwater circulation patterns. Atlantic-Pacific $\Delta\delta^{13}C$ and Indian-Pacific $\Delta\delta^{13}C$ records provide good proxies for the large-scale deepwater changes (Figure 8). Both the North Atlantic Ocean (Site 563, 3465 m) and the Indian Ocean (Site 237, 1337 m) recorded similarly high $\delta^{13}C$ values from 19 to 16 Ma, indicating that both regions were proximal to a source of high $\delta^{13}C$ water (Figure 8). This is even more evident in a time slice reconstruction at 16.2 Ma that shows high $\delta^{13}C$ values in both the deep North Atlantic and intermediate Indian oceans (Figure 9). These results reconcile the *Miller and Fairbanks* [1985] and *Woodruff and Savin* [1989] stud-

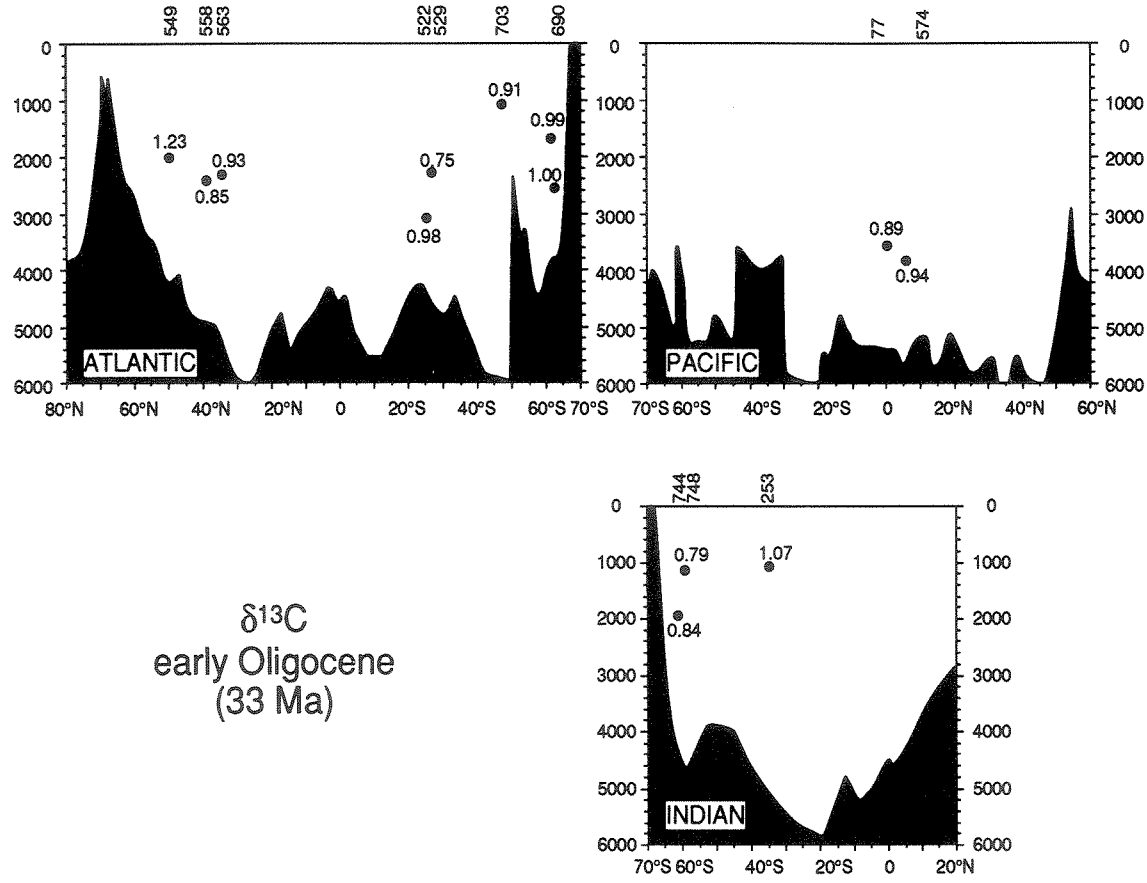

Fig. 7. Early Oligocene $\delta^{13}C$ cross section of the oceans at 33 Ma. As in the late Eocene, there is very little variation in the $\delta^{13}C$ values recorded throughout the oceans. This uniformity is attributed to low mean ocean nutrients and a vigorous deepwater source with a more central location. Again, there is a hint that an intermediate water mass was present in the North Atlantic (Site 549). This could reflect either Tethyan outflow or an intermediate branch of NCW. Stratigraphic levels and data sources for each site are listed in Table 1*b*.

ies, showing that both NCW and WSDW from the Tethys were produced during the early Miocene.

The convergence of North Atlantic and Pacific $\delta^{13}C$ records after 16 Ma suggests that NCW production ceased at this time (Figure 8). Interbasinal $\delta^{13}C$ differences redeveloped at about 12.5 Ma, indicating a renewal in NCW production. This is consistent with most Miocene deepwater circulation hypotheses [*Blanc et al.*, 1980; *Schnitker*, 1980; *Miller and Fairbanks*, 1985; *Woodruff and Savin*, 1989; *Wright et al.*, 1992]. Furthermore, most Miocene deepwater circulation scenarios suggest that NCW production remained high throughout the late Miocene, representing the evolution of modern deepwater circulation characteristics. *Wright et al.* [1991] concurred with this general picture; however, a high-resolution Southern Ocean $\delta^{13}C$ record indicates that there were higher-frequency fluctuations in NCW, occurring on the 10^5-year time scales (Figure 8). *Wright et al.* [1991] further noted that the absolute values and the differences in $\delta^{13}C$ among the North Atlantic, Pacific, and Southern oceans developed between 7 and 6 Ma in response to increased mean ocean nutrients and development of near-modern deepwater circulation patterns. A time slice reconstruction of the late Miocene (6 Ma; Figure 10) shows a pattern that was remarkably similar to the modern deepwater $\delta^{13}C$ distribution (Figure 3), suggesting that near-modern deepwater patterns operated during the late Miocene.

Oxygen Isotope Evidence

The Eocene was an interval of low benthic foraminiferal $\delta^{18}O$ values and high deepwater temperatures. Early Eocene deepwater temperatures were between 10° and 14°C, compared to today's 0°–2.5°C [*Shackleton and Kennett*, 1975; *Savin et al.*, 1975; *Miller et al.*, 1987]. Following peak warmth during the early Eocene, deep waters cooled by ~10° to 12°C over the next 16 m.y. as recorded by benthic foraminiferal $\delta^{18}O$ values which increased by ~3.0‰ [*Shackleton and Kennett*, 1975; *Savin et al.*, 1975; *Miller et al.*, 1987]. An initial increase of 1.0‰ occurred in the early middle Eocene

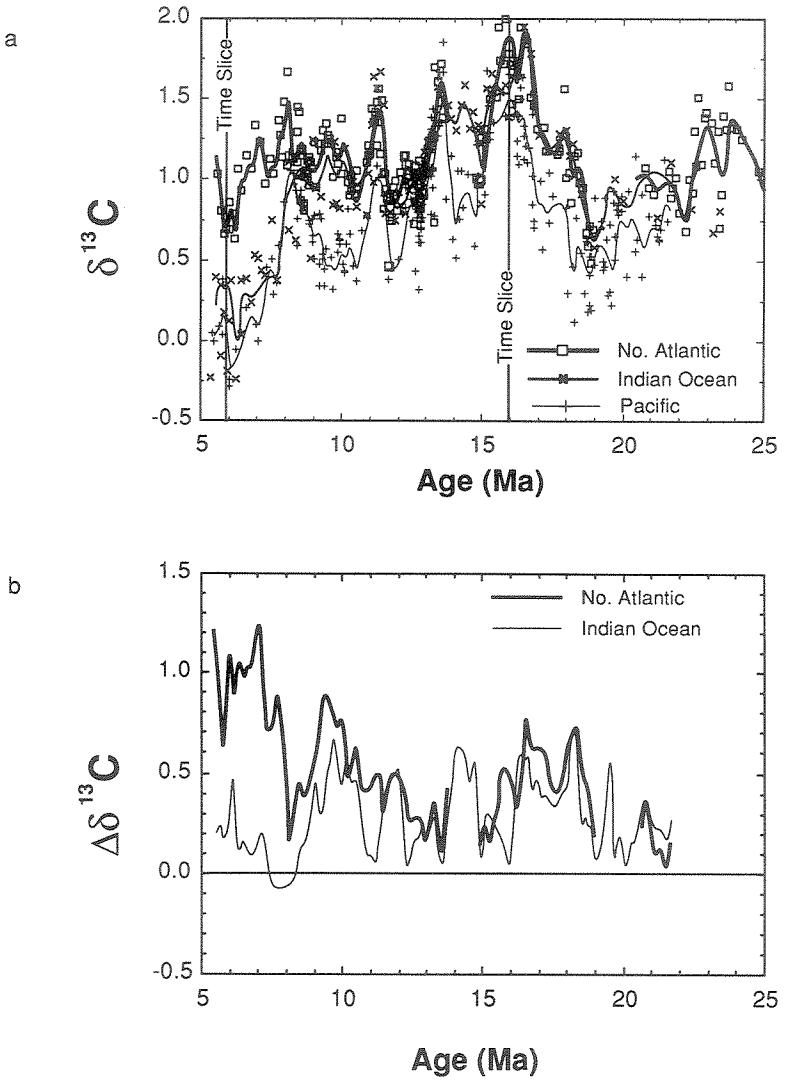

Fig. 8. (*a*) Miocene $\delta^{13}C$ records from the North Atlantic, Indian, and Pacific oceans. The smoothed lines for each record were generated by interpolating to a constant interval of 0.1 m.y. and using a five-point (0.25 m.y.) Gaussian filter. (*b*) To remove the mean ocean $\delta^{13}C$ changes which affected all sites, the smoothed Pacific record was subtracted from the North Atlantic and Indian Ocean records. High $\delta^{13}C$ values in the North Atlantic and Indian oceans relative to the Pacific Ocean indicate that the North Atlantic and Indian oceans were sources for deep to intermediate water masses from 20 to 16 Ma. Carbon isotope differences in the North Atlantic, Indian, and Pacific oceans were small between 16 and 12 Ma except for a brief interval in the Indian Ocean around 14 Ma. The small $\delta^{13}C$ contrast indicates that SCW was the dominant deepwater source during this interval. Interbasinal differences between the North Atlantic and Pacific oceans developed again by 12.5 Ma, indicating the renewal of NCW production. NCW production remained high through the late Miocene. Modern $\Delta\delta^{13}C$ differences between the Atlantic, Pacific, and Indian oceans developed by 7 Ma. Two $\delta^{13}C$ cross sections shown in Figures 9 and 10 are marked.

(52–49 Ma), followed by large, relatively rapid increases in the late middle Eocene (~0.75‰ at 43 Ma and ~0.75‰ at 40 Ma) and earliest Oligocene (~1‰ at 36 Ma; Figure 2). The $\delta^{18}O$ increases at 43 and 40 Ma preceded the apparent development of large ice sheets near the Eocene/Oligocene boundary, and therefore they are attributed to deepwater temperature decreases [e.g., *Miller*, 1992]. However, there is some evidence for possible glaciation during the late middle or late Eocene, and part of the increases could be attributed to ice volume changes [*Barron et al.*, 1991; *Robert and Maillott*, 1990; *Ehrmann*, 1991; *Ehrmann and Mackensen*, 1992].

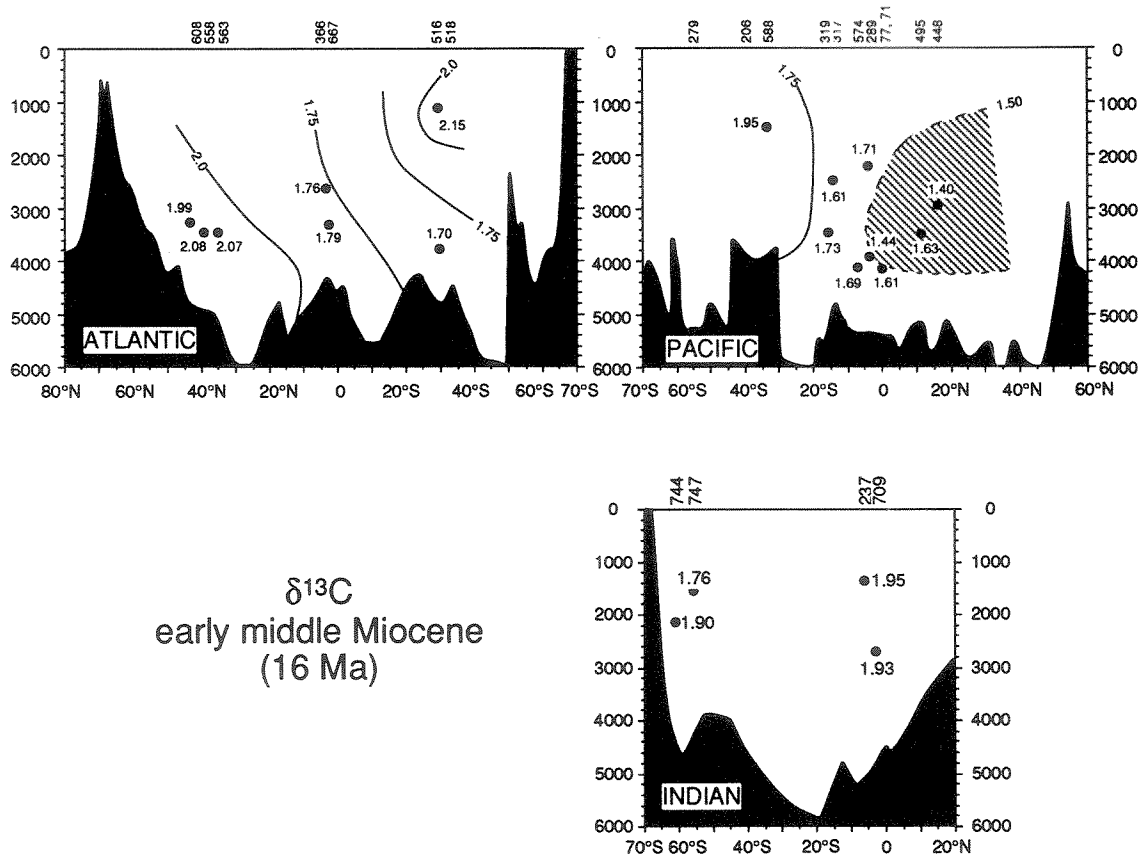

Fig. 9. Early/middle Miocene boundary $\delta^{13}C$ reconstruction (~16 Ma) [after *Wright et al.*, 1992]. The highest values were recorded in the deep North Atlantic and intermediate Indian oceans, indicating their proximity to deepwater sources, while the lowest values were still found in the Pacific. Stratigraphic levels and data sources for each site are listed in Table 1*c*.

Warm Eocene deepwater temperatures are consistent with WSDW production, although it is possible to ascribe these warm deep waters solely to polar warmth. *Shackleton and Boersma*'s [1981] Eocene reconstruction suggests that high-latitude surface waters were equally warm and, therefore, may have been a source of warm deep water (Figure 1). A more detailed reconstruction of Paleogene surface water $\delta^{18}O$ gradients compiled by *Zachos et al.* [1993] shows that planktonic and benthic foraminiferal $\delta^{18}O$ values were similar to each other in the high southern latitudes for much of the Paleogene. This observation has implications for deepwater sources because they acquire the temperature, salinity, and nutrient characteristics of the surface waters in regions of sinking. Similar $\delta^{18}O$ values in high-latitude planktonic and benthic foraminifera indicate that the temperature and salinity in the Southern Ocean were well mixed vertically, which is consistent with convection and a dominant southern ocean source. Alternatively, the similar values can be explained by low-salinity, low-$\delta^{18}O_{water}$ high-latitude surface waters that caused cool surface waters to appear warmer; however, this requires a serendipitous balance resulting in benthic and planktonic foraminifera recording the same $\delta^{18}O$ values, a hypothesis that we regard as unlikely. Carbon isotope data support a strong vertical link between the surface and deep waters in high latitudes because $\delta^{13}C$ records of planktonic and benthic foraminifera from Maud Rise [*Kennett and Stott*, 1990] and Kerguelen Plateau [*Barrera and Huber*, 1991] paralleled each other for much of the Paleogene.

An alternative explanation for similar planktonic and benthic $\delta^{18}O$ and $\delta^{13}C$ records in the Southern Ocean is that deep upwelling rather than deep convection caused the vertical mixing. Upwelled deep water can have a strong imprint on surface water characteristics, particularly in regions where there is a strong divergence in the surface waters, such as the modern Southern Ocean. However, given that many of the present-day markers for high Southern Ocean productivity (for example, high biogenic silica and high sedimentation rates) are poorly developed in the Paleogene of this region [*Barker et al.*,

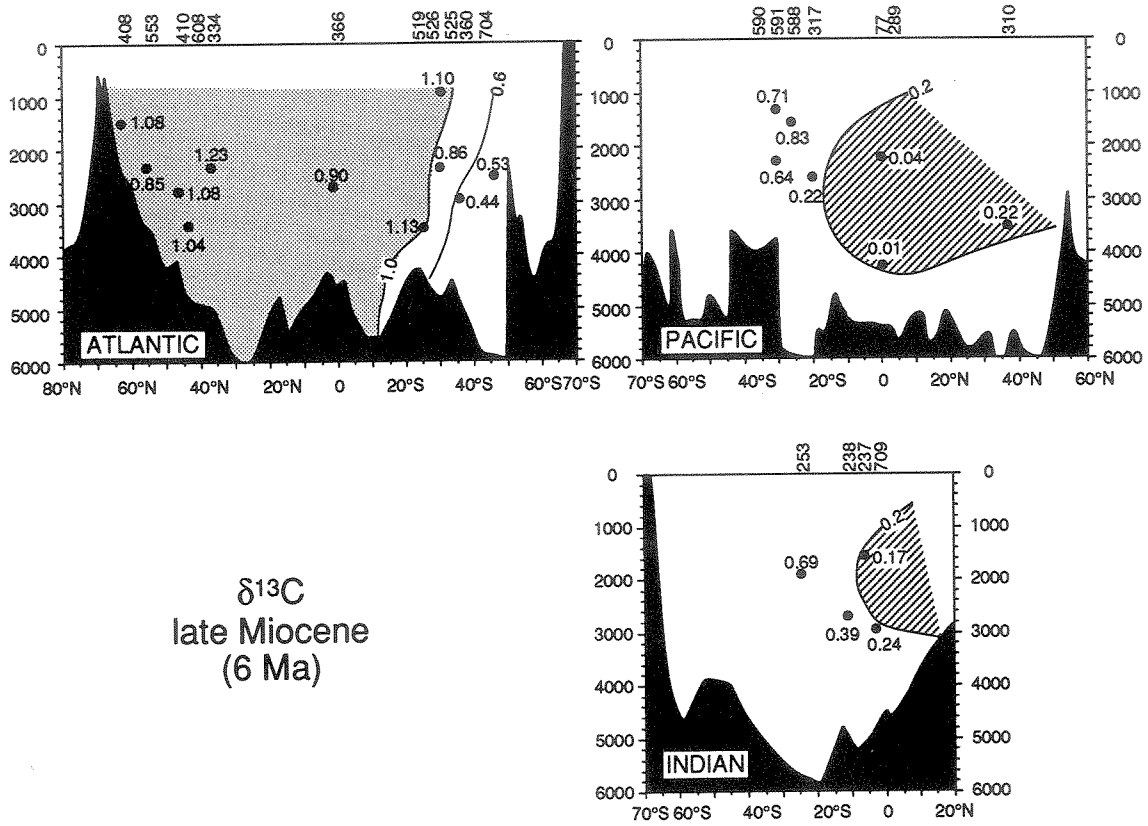

Fig. 10. Late Miocene $\delta^{13}C$ reconstruction (~6 Ma). The highest values were recorded in the deep North Atlantic, intermediate values were found in the Southern Ocean, and the lowest values were still found in the Pacific. The absolute values and distribution of $\delta^{13}C$ throughout the late Miocene ocean is strikingly similar to the modern. Stratigraphic levels and data sources for each site are listed in Table 1*d*.

1990; *Ciesielski et al.*, 1991; *Schlich et al.*, 1992], we regard this hypothesis as less likely.

Other oxygen isotope evidence from the Southern Ocean may indicate WSDW production during the Paleogene [*Kennett and Stott*, 1990]. Inversion of benthic foraminiferal $\delta^{18}O$ values on Maud Rise during the late Eocene through early Oligocene may reflect WSDW below a cooler, fresher intermediate water mass [*Kennett and Stott*, 1990]. Intermediate depth Site 689 (~1500-m paleodepth) recorded higher $\delta^{18}O$ values than the upper deepwater Site 690 (~2200 m) during this interval (Figure 2). The $\delta^{18}O$ difference between these sites averaged 0.5‰ but occasionally reached 1.0‰ (Figure 2) [*Kennett and Stott*, 1990]. The relatively higher $\delta^{18}O$ values at intermediate depths in the Southern Ocean are confirmed on the Kerguelen Plateau [*Barrera and Huber*, 1991]. If this $\delta^{18}O_{calcite}$ difference were based on temperature alone, then it would indicate a temperature inversion of 2°–4°C. *Kennett and Stott* [1990] noted that salinities must have been higher at greater depths to counter the warmer temperatures and maintain a plausible density contrast. The $\delta^{18}O_{water}$/salinity relationship for the ocean is positive; in other words, higher salinities correspond to higher $\delta^{18}O_{water}$ [*Craig and Gordon*, 1965]. Higher deepwater $\delta^{18}O_{water}$ values make $\delta^{18}O_{calcite}$ values appear to reflect colder temperatures. Therefore the 0.5 to 1.0‰ $\delta^{18}O$ differences must reflect a larger temperature difference than the previous 2°–4°C estimate [*Kennett and Stott*, 1990].

If the *Kennett and Stott* [1990] hypothesis is correct, then a "fingerprint" should exist in mid-latitude planktonic foraminiferal records. One would expect to find similar $\delta^{18}O$ and $\delta^{13}C$ values between these planktonic foraminifera and the benthic foraminifera as were found in the deep and high-latitude surface waters. There are no available records from the key areas (Tethys) to test this hypothesis. However, modeling efforts [*Barron*, 1987; *Rind and Chandler*, 1991] require a low- to mid-latitude flux of heat to the poles; if WSDW was not the source, then there should be evidence for greatly increased heat flux to the Southern Ocean through either surface currents or upwelling of intermediate water masses.

If we consider the Oligocene through Miocene, there is a strong correlation between deepwater temperatures

TABLE 1*a*. Data Used in the Late Eocene Time Slice Reconstruction (37.5 Ma)

Site	Depth, mbsf	Paleolatitude	Paleodepth	$\delta^{18}O$	$\delta^{13}C$	Source
			Atlantic			
522	151.99	26°S	2700	1.00	1.16	*Poore and Matthews* [1984]
549	134.76	49°N	2000	0.85	1.13	*Miller et al.* [1985]
690	93.95	65°S	2450	0.91	0.99	*Kennett and Stott* [1990]
702	21.33	51°S	2250	0.84	0.98	*Katz and Miller* [1992]
703	133.00	48°S	1000	0.78	1.14	*Miller* [1992]
			Pacific			
77	475.30	5°S	3200	0.60	1.01	*Keigwin and Keller* [1984]
574	518.50	2°S	3500	1.05	0.83	*Miller and Thomas* [1985]
			Indian			
738	32.84	59°S	1700	1.30	0.99	*Barrera and Huber* [1991]
744	156.07	58°S	1800	1.22	0.96	*Barrera and Huber* [1991]
748	123.80	54°S	1000	1.02	1.15	*Zachos et al.* [1992]

based on benthic foraminiferal $\delta^{18}O$ records and the production of NCW and WSDW that apparently controlled long-term variations (>1 m.y.) in deepwater temperatures [e.g., *Wright et al.*, 1992]. Benthic foraminiferal (*Cibicidoides*) $\delta^{18}O$ values fluctuated about a mean of 1.8‰ through the Oligocene and early Miocene. The constancy of the Oligocene $\delta^{18}O$ values relative to the Eocene and Miocene may be attributed to little change in deepwater sources. The $\delta^{13}C$ evidence indicates that SCW dominated deepwater production during the Oligocene. During the early Miocene, deep waters warmed by ~3°C between 19 and 16 Ma (Figure 11) [*Savin et al.*, 1975; *Shackleton and Kennett*, 1975; *Kennett and Shackleton*, 1976; *Wright et al.*, 1992]. The early Miocene deepwater temperature increase corresponded to increases in the NCW production [*Wright et al.*, 1992] and Tethyan outflow water [*Woodruff and Savin*, 1989]. Around 16 Ma, deepwater *Cibicidoides* spp. $\delta^{18}O$ values reached 1.0‰ in all three oceans and were the lowest recorded since the late Eocene. Deepwater temperatures are estimated to have been between 6° and 8°C at this time [*Shackleton and Kennett*, 1975; *Savin et al.*, 1975; *Wright et al.*, 1992]. Following peak warmth in the early middle Miocene, deep waters cooled by ~3°C as part of the middle Miocene $\delta^{18}O$ increase (15–12.5 Ma) (actually at least two steps, Mi3 and Mi4; Figure 11). The magnitude of this increase is attributed to a combination of ice growth and deepwater cooling (~3°C), both of which acted to increase the $\delta^{18}O$ value recorded in benthic foraminiferal calcite [*Shackleton and Kennett*, 1975; *Wright et al.*, 1992].

Higher-frequency $\delta^{18}O$ variations with durations of ~1 m.y. were superimposed on the long-term temperature trends. *Miller et al.* [1991] and *Wright and Miller*

TABLE 1*b*. Data Used in the Early Oligocene Time Slice Reconstruction (33 Ma)

Site	Depth, mbsf	Paleolatitude	Paleodepth	$\delta^{18}O$	$\delta^{13}C$	Source
			Atlantic			
522	108.30	26°S	3100	1.65	0.98	*Miller et al.* [1988]
529	158.13	28°S	2300	1.49	0.75	*Miller et al.* [1987]
549	107.43	49°N	2050	1.34	1.23	*Miller et al.* [1985]
558	391.35	38°N	2400	1.59	0.85	*Miller and Fairbanks* [1985]
563	346.04	34°N	2300	1.55	0.93	*Millet and Fairbanks* [1985]
689	110.95	64°S	1650	2.65	0.99	*Kennett and Stott* [1990]
690	90.20	65°S	2490	2.20	1.00	*Kennett and Stott* [1990]
703	99.88	48°S	1050	1.44	0.91	*Miller* [1992]
			Pacific			
77	442.08	4°S	3500	1.59	0.89	*Keigwin and Keller* [1984]
574	461.52	1°S	3850	1.53	0.94	*Miller and Thomas* [1985]
			Indian			
253	103.15	35°S	1050	1.36	1.07	*Oberhänsli* [1986]
744	128.67	58°S	1900	2.23	0.84	*Barrera and Huber* [1991]
748	105.60	55°S	1100	1.94	0.79	*Zachos et al.* [1992]

TABLE 1c. Data Used in the Early Middle Miocene Time Slice Reconstruction (16 Ma) [From *Wright et al.*, 1992]

Site	Depth, mbsf	Paleolatitude	Paleodepth	$\delta^{18}O$	$\delta^{13}C$	Source
			Atlantic			
366	159.23	6°N	2645	1.54	1.76	*Miller et al.* [1989]
516	93.98	30°S	1131	0.86	2.15	*Woodruff and Savin* [1989]
518	65.60	30°S	3746	1.69	1.70	*Woodruff and Savin* [1989]
558	292.31	38°N	3415	1.56	2.08	*Miller and Fairbanks* [1985]
563	248.93	34°N	3465	1.64	2.07	*Wright et al.* [1992]
608	331.40	43°N	3304	1.46	1.99	*Wright et al.* [1992]
667	183.66	5°N	3334	1.59	1.79	*Miller et al.* [1989]
			Pacific			
71	187.50	0°	4112	1.70	1.61	*Woodruff and Savin* [1989]
77	243.02	3.5°S	3910	1.44	1.44	*Savin et al.* [1981]; *Woodruff and Savin* [1989]
289	472.40	4.5°S	2307	1.55	1.71	*Savin et al.* [1981]; *Woodruff and Savin* [1989]
317	165.23	15°S	2519	1.87	1.61	*Woodruff and Savin* [1989]
319	107.40	16°S	3475	1.88	1.73	*Woodruff and Savin* [1989]
448	16.40	16°N	2938	1.46	1.40	*Woodruff and Savin* [1989]
495	236.90	12°N	3478	1.92	1.63	*Barrera et al.* [1985]
475	192.47	8°S	4158	1.98	1.69	*Woodruff and Savin* [1989]
588	314.30	32.5°S	1453	1.30	1.95	*Kennett* [1986]
			Indian			
237	159.20	9°S	1337	1.76	1.95	*Woodruff and Savin* [1989]
709	141.65	6°S	2744	1.78	1.93	*Woodruff et al.* [1990]
744	64.74	61°S	2125	1.90	1.90	*Woodruff and Chambers* [1991]
747	84.90	55°S	1532	1.42	1.76	*Wright and Miller* [1992]

TABLE 1d. Data Used in the Late Miocene Time Slice Reconstruction (6 Ma)

Site	Depth, mbsf	Paleolatitude	Paleodepth	$\delta^{18}O$	$\delta^{13}C$	Source
			Atlantic			
334	140.00	37°N	2350	2.29	1.23	*Keigwin et al.* [1986]
360	131.59	36°S	2975	2.47	0.44	*Wright et al.* [1991]
366	54.41	6°N	2765	2.89	0.90	*Stein* [1984]
408	100.76	63°N	1466	2.55	1.08	*Keigwin et al.* [1986]
410	175.10	45°N	2735	2.39	1.03	*Keigwin et al.* [1986]
519	111.20	26°S	3510	2.57	1.13	*McKenzie et al.* [1984]
525	22.20	29°S	2380	2.70	0.86	*Shackleton et al.* [1984]
526	49.22	30°S	975	2.41	1.10	*Shackleton et al.* [1984]
553	156.90	56°N	2310	2.25	0.85	*Wright et al.* [1992]
608	142.02	43°N	3470	2.23	1.04	*Wright et al.* [1991]
704	234.84	47°S	2550	2.71	0.53	*Wright et al.* [1991]
			Pacific			
77	92.27	2°S	4050	2.01	0.01	*Savin et al.* [1981]; *Woodruff and Savin* [1989]
289	167.08	2°S	2250	2.39	0.04	*Savin et al.* [1981]
310	60.50	35°N	3480	2.36	0.22	*Woodruff and Savin* [1989]
317	87.60	13°S	2600	2.46	0.51	*Woodruff and Savin* [1989]
588	136.80	28°S	1670	2.03	0.83	*Kennett* [1986]
590	227.60	33°S	1350	1.84	0.71	*Kennett* [1986]
591	240.70	33°S	2200	2.33	0.64	*Kennett* [1986]
			Indian			
237	86.04	8°S	1540	2.48	0.17	*Woodruff and Savin* [1989]
238	137.20	12°S	2740	2.39	0.39	*Vincent et al.* [1980]
253	28.00	27°S	1830	2.45	0.69	*Oberhänsli* [1986]
709	59.25	5°S	2950	2.62	0.24	*Woodruff et al.* [1990]
714	41.40	3°N	1925	2.09	0.55	*Boersma and Mikkelsen* [1990]

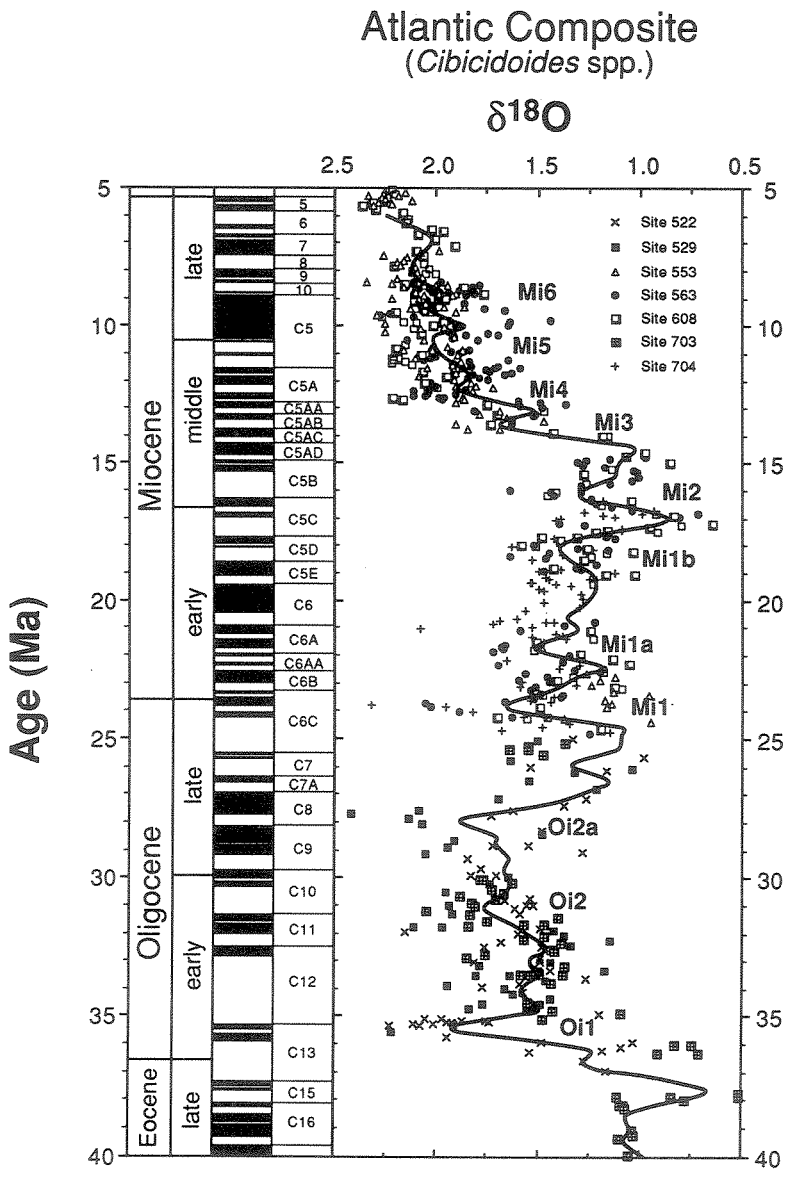

Fig. 11. Composite *Cibicidoides* $\delta^{18}O$ record for the Atlantic (redrawn from *Miller et al.* [1987]). The smoothed line was generated by interpolating the data to constant intervals of 0.1 m.y. and smoothing with a 21-point Gaussian filter. The Oligocene isotope ("Oi") and Miocene "Mi" zonations of *Miller et al.* [1991] and *Wright and Miller* [1992] are noted as "Oi" and "Mi" events. These benthic foraminiferal $\delta^{18}O$ increases covary with planktonic foraminiferal $\delta^{18}O$ increases and correlate with intervals of sediment deposition on and around Antarctica consistent with continental ice sheets [*Miller et al.*, 1991].

[1992] suggested that the $\delta^{18}O$ increases in their Oligocene and Miocene oxygen isotope zonations were caused by continental ice growth. They argued that planktonic-benthic foraminiferal $\delta^{18}O$ covariance indicates that these $\delta^{18}O$ increases reflected continental ice growth events followed by ice sheet melting [*Miller et al.*, 1991; *Wright et al.*, 1992]. There were three $\delta^{18}O$ maxima during the Oligocene that punctuated the long-term trend at ~36, 31, and 28 Ma (equal to bases of isotope zones Oi1, Oi2, and Oi2a) that reflected ice growth and decay on Antarctica (Figure 11). During the Miocene, global increases in $\delta^{18}O$ have been noted at ~24, 22, 20, 18, 16, 13.5, 12.5, 10, and 8 Ma (Figure 11) [*Miller et al.*, 1991]. These increases were interpreted as continental ice growth events as well.

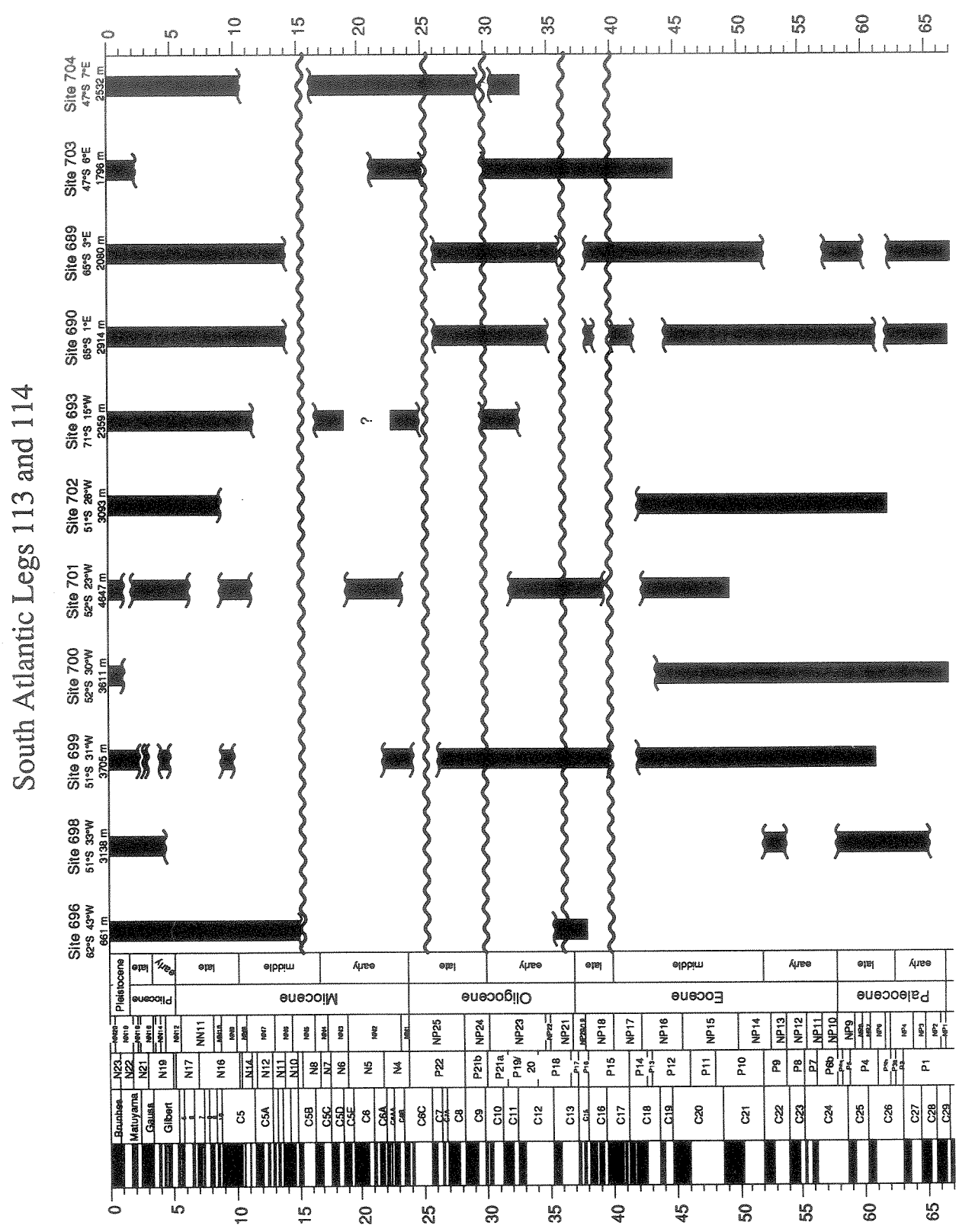

Fig. 12*a*. Cenozoic sediment accumulation at DSDP and ODP sites in the Southern Ocean for the Atlantic sector.

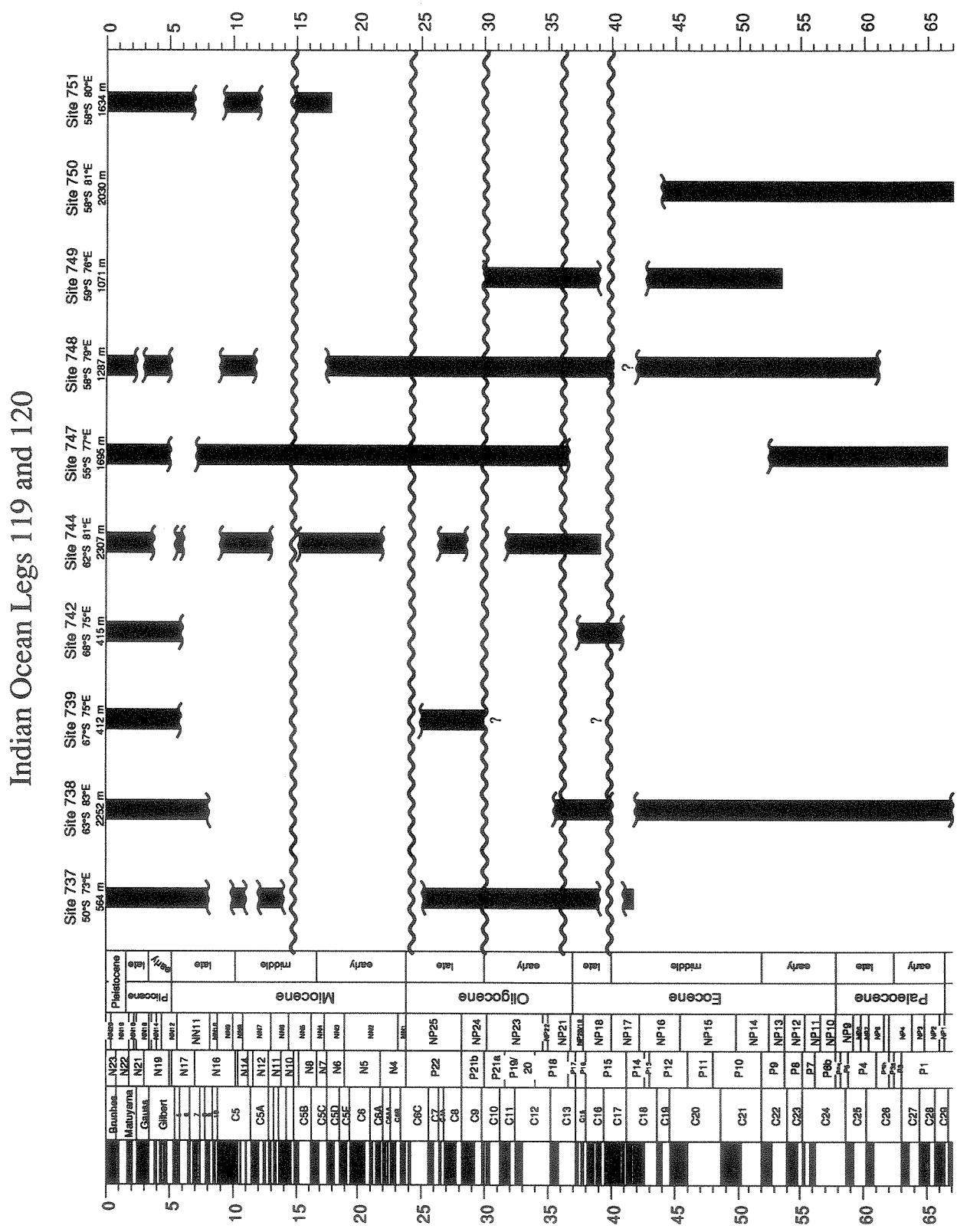

Fig. 12*b*. Cenozoic sediment accumulation at DSDP and ODP sites in the Southern Ocean for the Indian sector.

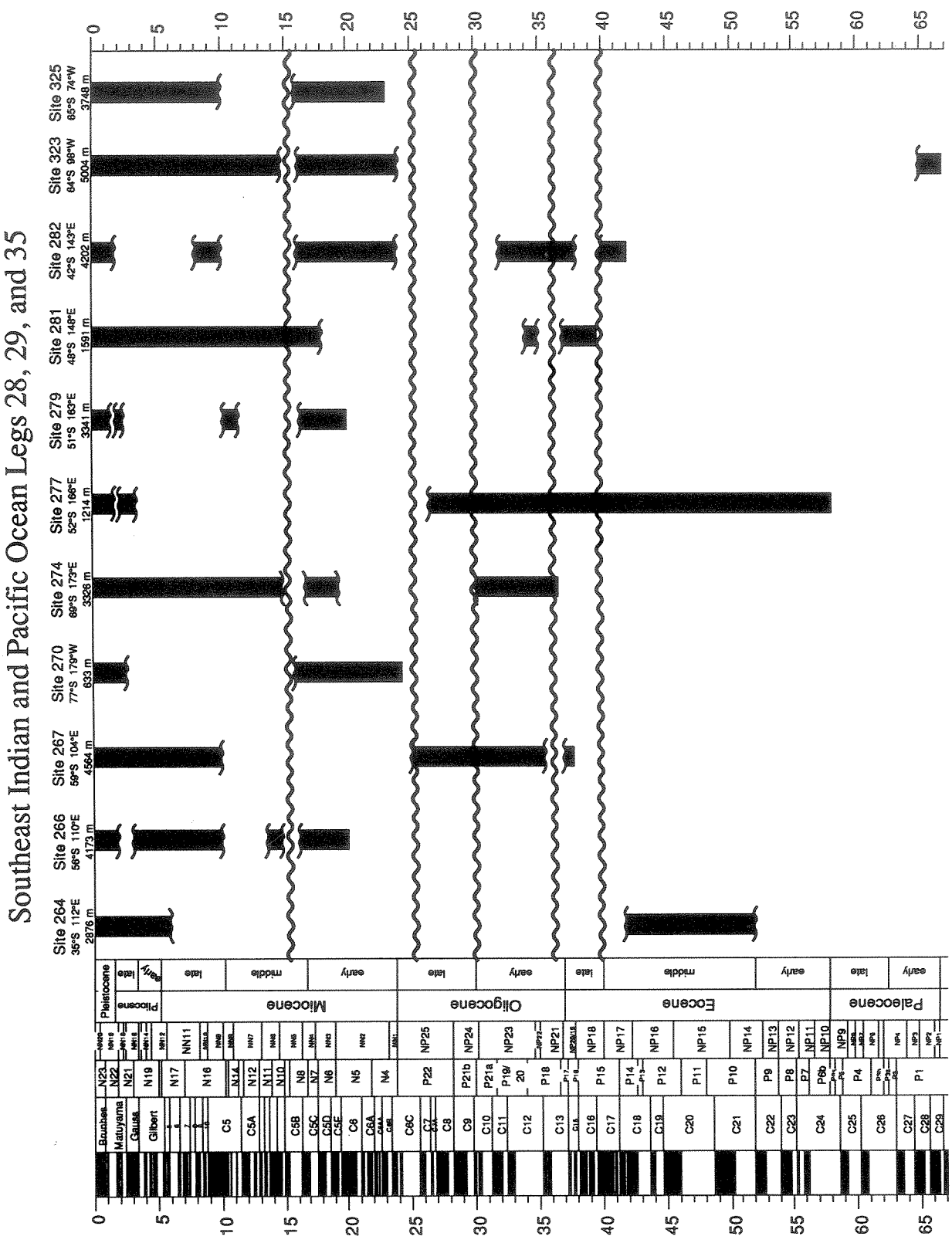

Fig. 12*c*. Cenozoic sediment accumulation at DSDP and ODP sites in the Southern Ocean for the Pacific sector.

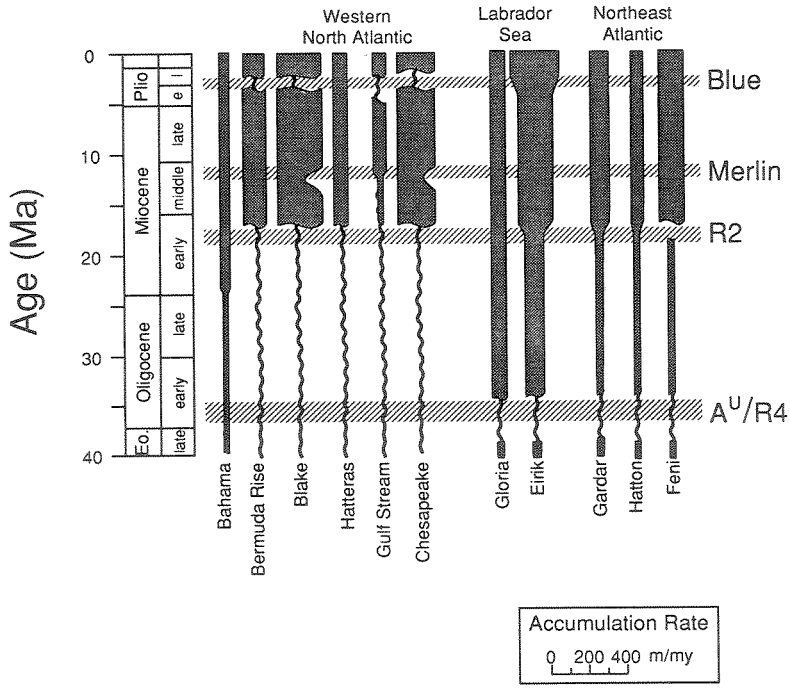

Fig. 13. The accumulation history of drift deposits in the North Atlantic during the Cenozoic (after G. S. Mountain and K. G. Miller, unpublished data). An extensive erosional unconformity (Reflector R4) in the northern North Atlantic occurred near the Eocene/Oligocene boundary and has been traced to the Greenland-Scotland Ridge [*Roberts*, 1975; *Miller and Tucholke*, 1983]. This unconformity is expressed as Reflector A^u in the western North Atlantic basins [*Miller and Tucholke*, 1983]. Following the initial pulse at 36 Ma, sediments accumulated in chaotic sequences before normal sedimentary features developed by 34 Ma. Two other erosional pulses follow by widespread drift accumulation occurred at 19 to 16 Ma [*Roberts* [1975]; Reflector R2) and 11.5 Ma (Reflector Merlin of *Mountain and Tucholke* [1985]). Each of these three erosional cycles correlate to subsidence on the Greenland-Scotland Ridge, which presumably allowed a dense water mass in the proto-Norwegian and Greenland seas to spill over into the northern North Atlantic.

Sediment Deposition and Erosion

The Southern Ocean. The late Eocene to early Oligocene climatic cooling led to an increase in the erosional capacity of bottom waters [*Kennett and Shackleton*, 1976]. *Kennett and Shackleton* [1976] noted that hiatuses in the Southern Ocean correspond to the $\delta^{18}O$ increase near the Eocene/Oligocene boundary (36 Ma). Drilling in the Southern Ocean during Ocean Drilling Program legs 113, 114, 119, and 120 [*Barker et al.*, 1990; *Barron et al.*, 1991; *Ciesielski et al.*, 1992; *Schlich et al.*, 1992] provides the foundation to reevaluate sediment distribution and hiatuses in the Southern Ocean.

The sedimentation record varies widely throughout the Cenozoic Southern Ocean (Figure 12). Even sites within close proximity to each other often show dissimilar patterns (for example, Maud Rise sites 689 and 690 [*Thomas et al.*, 1990; *Gersonde et al.*, 1990]). *Kennett and Stott* [1990] argued that differences in sedimentation patterns on Maud Rise resulted from the influence of two different water masses.

We identified five hiatuses that are prevalent, but not ubiquitous, in the Southern Ocean by compiling accumulation records by geographic region despite bathymetric differences in hiatus distributions. Each of these hiatuses corresponds to either an epochal boundary or epochal subdivision. These major erosional events occurred at (1) the middle/late Eocene boundary (~40 Ma), (2) the Eocene/Oligocene boundary (~36 Ma), (3) the early/late Oligocene boundary (~30 Ma), (4) the Oligocene/Miocene boundary (~24 Ma), and (5) near the early/middle Miocene boundary (~15 Ma) (Figure 12). We suggest that these Southern Ocean hiatuses resulted from increases in Southern Ocean deepwater production.

There appears to be a direct correlation between the periods of erosion in the Southern Ocean and global increases in the benthic foraminiferal $\delta^{18}O$ record. The earliest Oligocene and middle Miocene $\delta^{18}O$ increases are well established [*Shackleton and Kennett*, 1975; *Savin et al.*, 1975] and correspond to the erosional unconformities at 36 and 15 Ma [*Kennett and Shackleton*, 1976]. *Miller and Fairbanks* [1985] noted a large

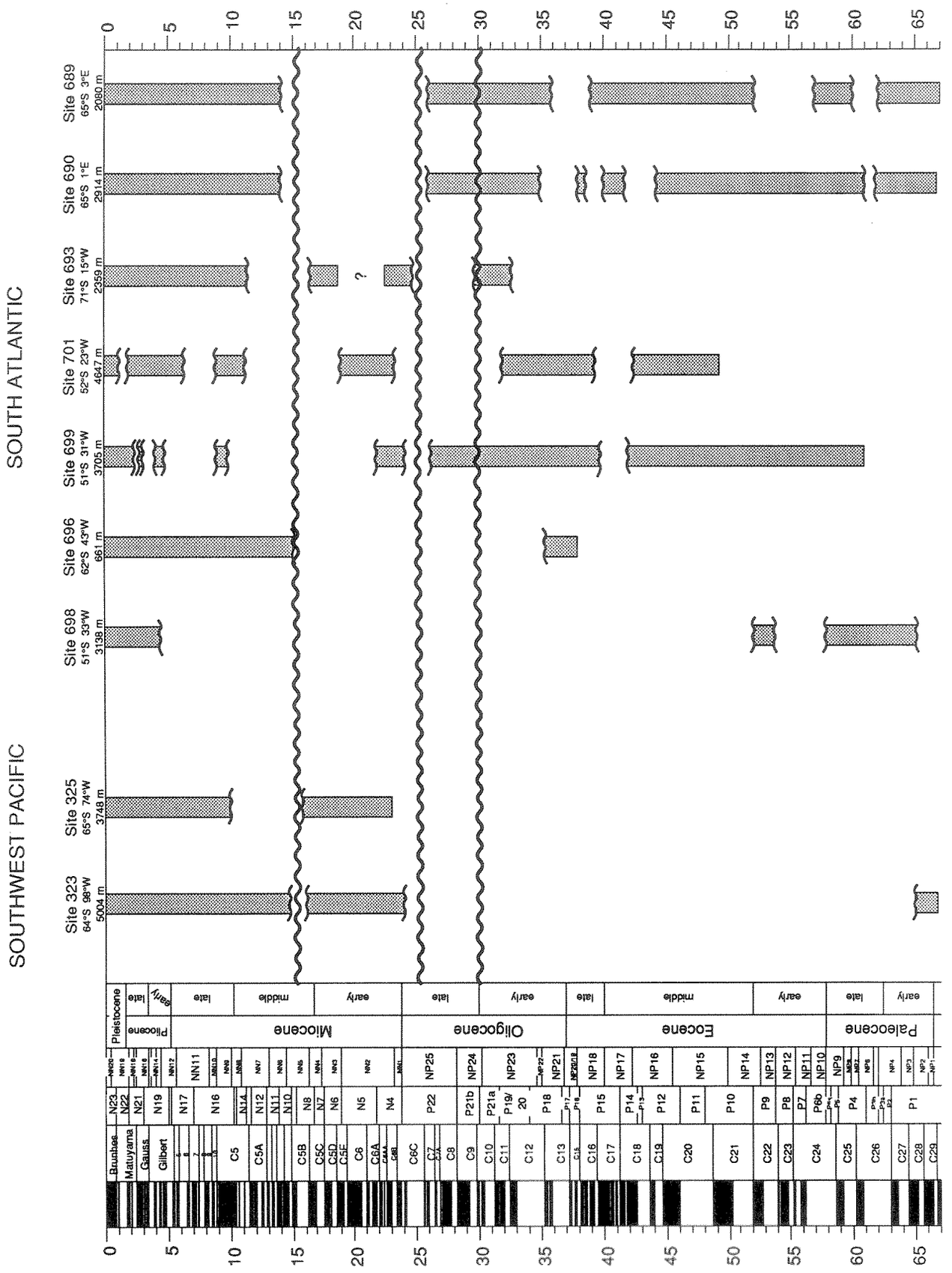

Fig. 14. Sediment accumulation at DSDP and ODP sites in the southeastern Pacific and southwestern Atlantic during the Cenozoic.

(>1‰) $\delta^{18}O$ increase at the Oligocene/Miocene boundary that is correlative to the unconformity of similar age (24 Ma). More recently, *Miller et al.* [1991] and *Wright and Miller* [1992] identified additional global $\delta^{18}O$ increases at 32, 28, 22, 18, and 16 Ma as part of their Oligocene and Miocene isotope zonations (Figure 11). Either the 32 or 28 Ma $\delta^{18}O$ increase could be related to the 30 Ma hiatus. The absence of lower Miocene sediments at several Southern Ocean sites may be related to a concatenation of hiatuses associated with the $\delta^{18}O$ increases at 22, 18, and 16 Ma (Figures 11 and 12).

Erosion in the Southern Ocean must reflect an increase in bottom current velocities. In a comparison of model simulations between early Cenozoic and present-day conditions, *Barron et al.* [1991] noted that the strength of SCW appeared to reflect the extent of Antarctic glaciation. Similarly, we suggest that the periodic growth or expansions of the Antarctica ice sheets increased the temperature gradient in the Southern Ocean, leading to more vigorous deepwater circulation originating in the Southern Ocean. This implies that there was a causal relationship between intervals of ice growth noted above, increased SCW production, and erosion.

North Atlantic Erosional and depositional patterns. Depositional patterns in the North Atlantic reflect large-scale deepwater circulation changes beginning in the earliest Oligocene through the middle Miocene. There is extensive evidence for the periodic development of strong deepwater currents with a North Atlantic source from the early Oligocene through middle Miocene [*Jones et al.*, 1970; *Ruddiman*, 1972; *Tucholke and Mountain*, 1979, 1986; *Miller and Tucholke*, 1983; *Mountain and Tucholke*, 1985; *Mountain and Miller*, 1992]. Uppermost Eocene to lowermost Oligocene reflectors R4 in the northern North Atlantic [*Roberts*, 1975; *Miller and Tucholke*, 1983] and A^u along the western edge of the North Atlantic [*Tucholke and Mountain*, 1979, 1986; *Mountain and Tucholke*, 1985; *Mountain and Miller*, 1992] resulted from erosional unconformities (Figure 13). These unconformities can be traced to the Greenland-Scotland Ridge, which is the source of northern deepwater currents. After this initial erosional pulse, large sediment drifts developed in the Labrador Sea and the northeast Atlantic (the Gloria, Eirik, Gardar, Hatton, and Feni drifts) (Figure 13).

The next change in drift deposition occurred in the early Miocene. *Roberts* [1975] identified Reflector R2 in the northern North Atlantic, which is a seismic disconformity with an age estimate of 20–16 Ma [*Ruddiman*, 1972; *Miller and Tucholke*, 1983; *Mountain and Tucholke*, 1985; *Wright et al.*, 1992]. The accumulation rates of North Atlantic drifts increased significantly following this erosional pulse. *Ruddiman* [1972] identified an erosional phase on the Reykjanes Ridge based on the pinchout of seismic reflectors. Following this erosional pulse, sedimentation accumulation increased significantly on the Reykjanes Ridge between 18 and 17 Ma. A third North Atlantic reflector, "Merlin," was identified by *Mountain and Tucholke* [1985] (Figure 13). The age of this event is constrained only to the late middle Miocene (~12–10 Ma). Since 10 Ma, sediment accumulation on the Reykjanes Ridge has reflected redeposition by nearly continuous deep currents [*Ruddiman*, 1972]. Each of these erosional events and subsequent drift depositions correlate to intervals of NCW production inferred from $\delta^{13}C$ reconstructions. The three major seismic disconformities (A^u/R4, R2, and Merlin) thus correspond to three intervals of large basin-basin $\delta^{13}C$ differences, ~35, 18–16 Ma, and 12–10 Ma. The corroboration of the $\delta^{13}C$ inferences and the seismic stratigraphy indicate that these intervals were of peak NCW flux.

Tectonics and Circumpolar Circulation

There is a direct link between climate, deepwater formation, and tectonics on time scales of a million years or longer [*Barron and Peterson*, 1991]. The gradual change from the quasi-circumequatorial circulation of the Cretaceous and early Paleogene to the development of circumpolar circulation may have been the fundamental cause behind the long-term trend toward colder polar climates during the Cenozoic [*Kennett and Shackleton*, 1976; *Kennett*, 1977; *Barron*, 1987; *Barron and Peterson*, 1991; *Kennett and Stott*, 1990]. *Kennett and Shackleton* [1976] and *Kennett* [1977] suggested that the development of the circumpolar circulation resulted in the thermal isolation of Antarctica from low-latitude heat sources. The removal of two tectonic barriers led to the initiation of circumpolar circulation. *Kennett et al.* [1974] noted that the deep subsidence of the Tasman Rise was a critical tectonic event for circumpolar circulation. They suggested that this occurred during the early to middle Oligocene based on sediment accumulation at DSDP sites from Leg 29, although subsequent work showed that the initial breakup between Antarctica and Australia began around 85 Ma (anomaly 34); normal seafloor spreading began at ~43 Ma (anomaly 19) [*Mutter et al.*, 1985].

The Drake Passage was the second physical barrier to circumpolar circulation. While most tectonic reconstructions of the Drake Passage suggest that it opened near the Oligocene/Miocene boundary [*Barker and Burrell*, 1977, 1982], the complexity of the Drake Passage precludes any model which is based on identifying magnetic anomalies in the Scotia Sea [*Lawver et al.*, 1992]. Shallow connections may have developed between the South Atlantic and Pacific oceans as the tip of South America moved to the east past the Antarctic peninsula near the Eocene/Oligocene boundary, independent of the opening of the Scotia Sea [*Lawver et al.*, 1992]. On the basis of southeast Pacific sedimentation (Deep Sea Drilling Project (DSDP) Leg 35), *Tucholke et al.* [1976] speculated that the initial breach of the Drake

Passage occurred between the late Eocene and early Oligocene, allowing a shallow circumpolar current to develop. The timing of the evolution of deep circumpolar circulation is less certain. *Barker and Burrell* [1982] suggested that the deep connection through the Scotia Sea developed near the Oligocene/Miocene boundary. Sediment accumulation patterns in the South Atlantic and southeast Pacific show a prominent hiatus near 24 Ma (Figure 14). For example, at Site 323 in the southeast Pacific, lower Miocene terrigenous silts and clays that indicate current-controlled deposition were deposited on Danian pelagic sediments. This unconformity was interpreted to reflect a strong deepwater current that developed near the Oligocene/Miocene boundary and eroded the sediment record back to the Cretaceous [*Tucholke et al.*, 1976]. Our compilation (Figures 12 and 14) (1) is consistent with a shallow opening of the Drake Passage by the earliest Oligocene, which triggered further isolation and consequent glaciation, and (2) argues for a distinct erosional event near the Oligocene/Miocene boundary which we attribute to opening of the deep passages.

CONCLUSIONS

The long-term fluctuations in deepwater temperatures responded to the WSDW production during the Cenozoic. Most of the evidence for deepwater circulation patterns presented here indicates that the Southern Ocean has been the dominant deepwater source for the past 40 m.y.:

1. Relatively high benthic foraminiferal $\delta^{13}C$ values were recorded in the Southern Ocean during much of the late Eocene to early Miocene, indicating that this region was proximal to a deepwater source.
2. Relatively high global deepwater $\delta^{18}O$ values are interpreted as cold temperatures, particularly during the Oligocene and the middle Miocene to Recent (see also *Shackleton and Kennett* [1976] and *Kennett and Stott* [1990]).
3. Similar $\delta^{18}O$ values recorded in benthic and high-latitude planktonic foraminiferal records throughout the late Eocene to Recent are consistent with, but are not indisputable proof for deep convection in the Southern Ocean.
4. Late Eocene (~40 Ma), earliest Oligocene (~36 Ma), middle Oligocene (~30 Ma), latest Oligocene (~24 Ma), and middle Miocene (~15 Ma) hiatuses occurred at many Southern Ocean sites, indicating increases in Southern Ocean bottom water currents.

A $\delta^{18}O_{calcite}$ inversion at Maud Rise may reflect the presence of WSDW below a colder, fresher water mass [*Kennett and Stott*, 1990], providing evidence for WSDW in the Paleogene oceans. It remains unclear whether WSDW contributed heat and salt to the deepwater masses by directly filling the deep oceans or through a poleward flux that surfaced in the high southern latitudes and was redistributed by SCW. In either case, a colder and fresher intermediate water mass originated in the Southern Ocean, producing the $\delta^{18}O$ inversion during the late Eocene to Oligocene.

Although SCW generally dominated the Oligocene, there is evidence from carbon isotopes, seismic stratigraphy, and hiatuses that indicate that a pulse of NCW occurred in the earliest Oligocene. Miocene deepwater circulation patterns occurred in two cycles. The first began in the earliest Miocene with a one-component deepwater system dominated by SCW. NCW and Tethyan outflow water production supplemented SCW production between 19 and 16 Ma. The production of NCW and Tethyan outflow water was reduced between 16 and 15 Ma, leaving SCW as the dominant deepwater mass ventilating the deep oceans. At about 12.5 Ma, $\delta^{13}C$ reconstructions indicate that NCW production was renewed and continued through the late Miocene when near-modern deepwater circulation patterns developed.

Acknowledgments. G. Brass, M. Katz, J. Kennett, G. Mead, and L. Stott provided critical reviews which greatly improved this manuscript. This manuscript also benefited from discussions with C. Charles, R. Fairbanks, J. Lynch-Stieglitz, D. Pak, and L. Burckle. This work was supported by National Science Foundation grant OCE88-11834 to K.G.M. and grant OCE91-17667 to J.D.W. This is Lamont-Doherty Geological Observatory contribution 5027.

REFERENCES

Barker, P. F., and J. Burrell, The opening of Drake Passage, *Mar. Geol.*, *25*, 15–34, 1977.

Barker, P. F., and J. Burrell, The influence upon Southern Ocean circulation, sedimentation, and climate of the opening of Drake Passage, in *Antarctic Geoscience*, edited by C. Craddock, pp. 377–385, University of Wisconsin Press, Madison, 1982.

Barker, P. F., et al., Leg 113, *Proc. Ocean Drill. Program Sci. Results*, *113*, 1033 pp., 1990.

Barrera, E., and B. T. Huber, Paleogene and early Neogene oceanography of the southern Indian Ocean: Leg 119 foraminifer stable isotope results, *Proc. Ocean Drill. Program Sci. Results*, *119*, 693–717, 1991.

Barrera, E., G. Keller, and S. M. Savin, Evolution of the Miocene ocean in the eastern North Pacific as inferred from oxygen and carbon isotopic ratios of foraminifera, The Miocene Ocean: Paleoceanography and Biogeography, *Mem. Geol. Soc. Am.*, *163*, 83–102, 1985.

Barron, E. J., A warm, equable Cretaceous: The nature of the problem, *Earth Sci. Rev.*, *19*, 305–338, 1983.

Barron, E. J., Eocene equator-to-pole surface ocean temperatures: A significant climate problem?, *Paleoceanography*, *2*, 729–739, 1987.

Barron, E. J., and W. H. Peterson, The Cenozoic ocean circulation based on ocean General Circulation Model results, *Palaeogeogr. Palaeoclimatol. Palaeoecol.*, *83*, 1–28, 1991.

Barron, J. A., et al., Leg 119, *Proc. Ocean Drill. Program Sci. Results*, *119*, 1003 pp., 1991.

Belanger, P. E., W. B. Curry, and R. K. Matthews, Core-top evaluation of benthic foraminiferal isotopic ratios for paleoceanographic interpretations, *Palaeogeogr. Palaeoclimatol. Palaeoecol.*, *33*, 205–220, 1981.

Bender, M. L., and D. W. Graham, On late Miocene abyssal hydrography, *Mar. Micropaleontol., 6*, 451–464, 1981.

Berggren, W. A., D. V. Kent, and J. A. Van Couvering, Neogene geochronology and chronostratigraphy, in *The Chronology of the Geological Record, Mem. 10*, edited by N. J. Snelling, pp. 211–260, Geological Society of London, London, 1985.

Blanc, P.-L., D. Rabussier, C. Vergnaud-Grazzini, and J. C. Duplessy, North Atlantic Deep Water formed by the later middle Miocene, *Nature, 283*, 553–555, 1980.

Boersma, A., and N. Mikkelsen, Miocene-age primary productivity episodes and oxygen minima in the central equatorial Indian Ocean, *Proc. Ocean Drill. Program Sci. Results, 115*, 589–610, 1990.

Boersma, A., I. Premoli Silva, and N. J. Shackleton, Atlantic Eocene planktonic foraminiferal paleohydrographic indicators and stable isotope paleoceanography, *Paleoceanography, 2*, 287–331, 1987.

Boyle, E. A., The role of vertical chemical fractionation in controlling late Quaternary atmospheric carbon dioxide, *J. Geophys. Res., 93*, 15,701–15,714, 1988.

Boyle, E. A., and L. D. Keigwin, Deep circulation of the North Atlantic over the last 200,000 years, geochemical evidence, *Science, 218*, 784–787, 1982.

Boyle, E. A., and L. D. Keigwin, North Atlantic thermohaline circulation during the past 20,000 years linked to high-latitude surface temperature, *Nature, 330*, 35–40, 1987.

Brass, G. W., J. R. Southam, and W. H. Peterson, Warm saline bottom water in the ancient ocean, *Nature, 296*, 620–623, 1982.

Broecker, W. S., A revised estimate for the radiocarbon age of North Atlantic Deep Water, *J. Geophys. Res., 84*, 3218–3226, 1979.

Broecker, W. S., Some thoughts about the radiocarbon budget of the glacial Atlantic, *Paleoceanography, 4*, 213–220, 1989.

Broecker, W. S., and T.-H. Peng, *Tracers in the Sea*, 690 pp., Eldigio, Palisades, N. Y., 1982.

Broecker, W. S., M. Andree, G. Bonani, W. Wolfli, H. Oeschger, M. Klas, A. Mix, and W. Curry, Preliminary estimates for the radiocarbon age of deep water in the glacial ocean, *Paleoceanography, 3*, 659–669, 1988.

Cande, S. C., and D. V. Kent, A new geomagnetic polarity time scale for the Late Cretaceous and Cenozoic, *J. Geophys. Res., 97*, 13,917–13,951, 1992.

Chamberlin, T. C., On a possible reversal of deep-sea circulation and its influence on geologic climates, *J. Geol., 14*, 363–373, 1906.

Charles, C. D., and R. G. Fairbanks, Evidence from Southern Ocean sediments for the effect of North Atlantic deep-water flux on climate, *Nature, 355*, 416–419, 1992.

Ciesielski, P. F., et al., Leg 114, *Proc. Ocean Drill. Program Sci. Results, 114*, 826 pp., 1991.

Covey, C., and E. Barron, The role of ocean heat transport in climatic change, *Earth Sci. Rev., 24*, 429–445, 1988.

Covey, C., and S. L. Thompson, Testing the effects of ocean heat transport on climate, *Global Planet. Change, 1*, 331–341, 1989.

Craig, H., and L. Gordon, Deuterium and oxygen-18 variations in the ocean and the marine atmosphere, in *Symposium of Marine Geochemistry, Publ. 3*, 277 pp., Graduate School of Oceanography, University of Rhode Island, Kingston, 1965.

Curry, W. B., and G. P. Lohmann, Carbon isotopic changes in benthic foraminifera from the western South Atlantic: Reconstruction of glacial abyssal circulation patterns, *Quat. Res., 18*, 218–235, 1982.

Curry, W. B., J.-C. Duplessy, L. D. Labeyrie, and N. J. Shackleton, Quaternary deep-water circulation changes in the distribution of $\delta^{13}C$ of deep water $\sum CO_2$ between the last glaciation and the Holocene, *Paleoceanography, 3*, 317–341, 1988.

Duplessy, J.-C., C. Lalou, and A. C. Vinot, Differential isotopic fractionation in benthic foraminifera and paleotemperatures reassessed, *Science, 168*, 250–251, 1970.

Duplessy, J.-C., N. J. Shackleton, R. G. Fairbanks, L. Labeyrie, D. Oppo, and N. Kallel, Deep-water source variations during the last climatic cycle and their impact on the global deepwater circulation, *Paleoceanography, 3*, 343–360, 1988.

Erhmann, W. U., Implications of sediment composition on the southern Kerguelen Plateau for paleoclimate and depositional environment, *Proc. Ocean Drill. Program Sci. Results, 119*, 185–210, 1991.

Erhmann, W. U., and A. Mackensen, Sedimentological evidence for the formation of an East Antarctic ice sheet tin Eocene/Oligocene time, *Palaeogeogr. Palaeoclimatol. Palaeoecol., 93*, 85–112, 1992.

Gersonde, R., et al., Biostratigraphic synthesis of Neogene siliceous microfossils for the Antarctic Ocean ODP Leg 113 (Weddell Sea), *Proc. Ocean Drill. Program Sci. Results, 113*, 915–936, 1990.

Graham, D. W., B. H. Corliss, M. L. Bender, and L. D. Keigwin, Carbon and oxygen isotopic disequilibria of Recent benthic foraminifera, *Mar. Micropaleontol., 6*, 483–497, 1981.

Haq, B., Paleogene paleoceanography: Early Cenozoic ocean revisited, *Oceanol. Acta, SP*, 71–82, 1981.

Jones, E. J., M. Ewing, J. I. Ewing, and S. L. Ettreim, Influences of Norwegian Sea overflow water on sedimentation in the northern North Atlantic and Labrador Sea, *J. Geophys. Res., 75*, 1655–1680, 1970.

Katz, M. E., and K. G. Miller, Early Paleogene benthic foraminiferal assemblages and stable isotopes in the Southern Ocean, *Proc. Ocean Drill. Program Sci. Results, 120*, 481–512, 1992.

Keigwin, L. D., and G. Keller, Middle Oligocene cooling from equatorial Pacific DSDP Site 77B, *Geology, 12*, 16–19, 1984.

Keigwin, L. D., M.-P. Aubry, and D. V. Kent, North Atlantic late Miocene stable-isotope stratigraphy, biostratigraphy, and magnetostratigraphy, *Initial Rep. Deep Sea Drill. Proj., 94*, 935–963, 1986.

Kennett, J. P., Cenozoic evolution of Antarctic glaciation, the Circum-Antarctic Ocean, and their impact on global paleoceanography, *J. Geophys. Res., 82*, 3843–3860, 1977.

Kennett, J. P., Miocene to early Pliocene oxygen and carbon isotope stratigraphy in the southwest Pacific, Deep Sea Drilling Project Leg 90, *Initial Rep. Deep Sea Drill. Proj., 90*, 1383–1411, 1986.

Kennett, J. P., and N. J. Shackleton, Oxygen isotopic evidence for the development of the psychrospheric 38 Myr. ago, *Nature, 260*, 513–515, 1976.

Kennett, J. P., and L. D. Stott, Proteus and Proto-Oceanus: Paleogene oceans as revealed from Antarctic stable isotopic results: ODP Leg 113, *Proc. Ocean Drill. Program Sci. Results, 113*, 865–880, 1990.

Kennett, J. P., et al., Development of the Circum-Antarctic Current, *Nature, 186*, 144–147, 1974.

Kroopnick, P., The distribution of ^{13}C of $\sum CO_2$ in the world oceans, *Deep Sea Res., 32*, 57–84, 1985.

Lawver, L. A., L. M. Gahagan, and M. F. Coffin, The development of paleoseaways around Antarctica, in *The Antarctic Paleoenvironment: A perspective on Global Change, Part 1, Antarct. Res. Ser.*, vol. 56, edited by J. P. Kennett and D. A. Warnke, pp. 7–30, AGU, Washington, D. C., 1992.

Manabe, S., and K. Bryan, Jr., CO_2-induced change in a coupled ocean-atmosphere model and its paleoclimatic implications, *J. Geophys. Res., 90*, 11,689–11,707, 1985.

Manabe, S., K. Bryan, Jr., and M. J. Spelman, Transient

response of a global ocean-atmosphere model to a doubling of atmospheric carbon dioxide, *J. Phys. Oceanogr.*, *20*, 722–749, 1990.

McKenzie, J. A., H. Weissert, R. Z. Poore, R. C. Wright, S. F. Percival, Jr., H. Oberhänsli, and M. Casey, Paleoceanographic implications of stable-isotope data from upper Miocene-lower Pliocene sediments from the southeast Atlantic (Deep Sea Drilling Project Site 519), *Initial Rep. Deep Sea Drill. Proj.*, *73*, 717–735, 1984.

Miller, K. G., Middle Eocene to Oligocene stable isotopes, climate, and deep-water history: The terminal Eocene event?, in *Eocene-Oligocene Climatic and Biotic Evolution*, edited by D. Prothero and W. A. Berggren, pp. 160–177, Princeton University, Princeton, N. J., 1992.

Miller, K. G., and R. G. Fairbanks, Evidence for Oligocene–middle Miocene abyssal circulation changes in the western North Atlantic, *Nature*, *306*, 250–253, 1983.

Miller, K. G., and R. G. Fairbanks, Oligocene to Miocene carbon isotope cycles and abyssal circulation changes, in *The Carbon Cycle and Atmospheric CO_2: Natural Variations Archean to Present*, *Geophys. Monogr. Ser.*, vol. 32, edited by E. T. Sundquist and W. S. Broecker, pp. 469–486, AGU, Washington, D. C., 1985.

Miller, K. G., and E. Thomas, Late Eocene to Oligocene benthic foraminiferal isotopic record, Site 574, equatorial Pacific, *Initial Rep. Deep Sea Drill. Proj.*, *85*, 771–777, 1985.

Miller, K. G., and B. E. Tucholke, Development of Cenozoic abyssal circulation south of the Greenland-Scotland Ridge, in *Structure and Development of the Greenland-Scotland Ridge*, edited by M. H. P. Bott, S. Saxov, M. Talwani, and J. Thiede, pp. 549–589, Plenum, New York, 1983.

Miller, K. G., W. B. Curry, and D. R. Ostermann, Late Paleogene (Eocene to Oligocene) benthic foraminiferal oceanography of the Goban Spur Region, Leg 80, *Initial Rep. Deep Sea Drill. Proj.*, *80*, 505–538, 1985.

Miller, K. G., R. G. Fairbanks, and G. S. Mountain, Tertiary oxygen isotope synthesis, sea level history, and continental margin erosion, *Paleoceanography*, *2*, 1–19, 1987.

Miller, K. G., M. D. Feigenson, D. V. Kent, and R. K. Olsson, Oligocene stable isotope ($^{87}Sr/^{86}Sr$, $\delta^{18}O$, $\delta^{13}C$) standard section, Deep Sea Drilling Project Site 522, *Paleoceanography*, *3*, 223–233, 1988.

Miller, K. G., J. D. Wright, and R. G. Fairbanks, Unlocking the icehouse: Oligocene-Miocene oxygen isotope, eustasy, and margin erosion, *J. Geophys. Res.*, *96*, 6829–6848, 1991.

Moore, T. C., T. H. van Andel, C. Sancetta, and N. Pisias, Cenozoic hiatuses in pelagic sediments, *Micropaleontology*, *24*, 113–138, 1978.

Mountain, G. S., and K. G. Miller, Seismic and geologic evidence for early Paleogene circulation in the western North Atlantic, *Paleoceanography*, *7*, 423–440, 1992.

Mountain, G. S., and B. E. Tucholke, Mesozoic and Cenozoic geology of the U.S. Atlantic continental slope and rise, in *Geologic Evolution of the United States Atlantic Margin*, edited by C. W. Poag, pp. 293–341, Van Nostrand Reinhold, New York, 1985.

Mutter, J. C., K. A. Hegarty, S. C. Cande, and J. K. Weissel, Breakup between Australia and Antarctica: A brief review in the light of new data, *Tectonophysics*, *114*, 255–279, 1985.

Oberhänsli, H., Latest Cretaceous–early Neogene oxygen and carbon isotopic record at DSDP sites in the Indian Ocean, *Mar. Micropaleontol.*, *10*, 91–115, 1986.

Oppo, D. W., and R. G. Fairbanks, Variability in the deep and intermediate water circulation of the Atlantic Ocean during the past 25,000 years: Northern hemisphere modulation of the Southern Ocean, *Earth Planet. Sci. Lett.*, *86*, 1–15, 1987.

Oppo, D. W., R. G. Fairbanks, and A. L. Gordon, Late Pleistocene Southern Ocean $\delta^{13}C$ variability, *Paleoceanography*, *5*, 43–54, 1990.

Pak, D. K., and K. G. Miller, Paleocene to Eocene benthic foraminiferal isotopes and assemblages: Implications for deepwater circulation, *Paleoceanography*, *7*, 405–422, 1992.

Poore, R. Z., and R. K. Matthews, Late Eocene–Oligocene oxygen and carbon isotope record from South Atlantic Ocean, *Initial Rep. Deep Sea Drill. Proj.*, *73*, 725–735, 1984.

Rind, D., The doubled CO_2 climate: Impact of the sea surface temperature gradient, *Am. J. Atmos. Sci.*, *44*, 3235–3268, 1987.

Rind, D., and M. Chandler, Increased ocean heat transports and warmer climate, *J. Geophys. Res.*, *96*, 7437–7461, 1991.

Robert, C., and H. Maillot, Paleoenvironments in the Weddell Sea area and Antarctic climates, as deduced from clay mineral associations and geochemical data, ODP Leg 113, *Proc. Ocean Drill. Program Sci. Results*, *113*, 51–70, 1990.

Roberts, D. G., Marine geology of the Rockall Plateau and Trough, *Philos. Trans. R. Soc. London, Ser. A*, *278*, 447–590, 1975.

Ruddiman, W. F., Sediment redistribution on the Reykjanes Ridge: Seismic evidence, *Geol. Soc. Am. Bull.*, *83*, 2039–2062, 1972.

Savin, S. M., R. G. Douglas, and F. G. Stehli, Tertiary marine paleotemperatures, *Geol. Soc. Am. Bull.*, *86*, 1499–1510, 1975.

Savin, S. M., G. Keller, R. G. Douglas, J. S. Killingley, L. Shaughnessy, M. A. Sommer, E. Vincent, and F. Woodruff, Miocene benthic foraminiferal isotope records: A synthesis, *Mar. Micropaleontol.*, *6*, 423–450, 1981.

Schlich, R., et al., Leg 120, *Proc. Ocean Drill. Program Sci. Results*, *120*, 1145 pp., 1992.

Schnitker, D., North Atlantic oceanography as possible cause of Antarctic glaciation and eutrophication, *Nature*, *284*, 615–616, 1980.

Shackleton, N. J., and A. Boersma, The climate of the Eocene ocean, *J. Geol. Soc. London*, *138*, 153–157, 1981.

Shackleton, N. J., and J. P. Kennett, Paleotemperature history of the Cenozoic and initiation of Antarctic glaciation: Oxygen and carbon isotopic analyses in DSDP sites 277, 279, and 281, *Initial Rep. Deep Sea Drill. Proj.*, *29*, 743–755, 1975.

Shackleton, N. J., and N. D. Opdyke, Oxygen isotope and paleomagnetic stratigraphy of equatorial Pacific Core V28-238: Oxygen isotope temperatures and ice volumes on a 10^5 year and 10^6 year scale, *Quat. Res.*, *3*, 39–55, 1973.

Shackleton, N. J., J. Imbrie, and M. A. Hall, Oxygen and carbon isotope record of East Pacific Core V19-30: Implications for the formation of deep water in the late Pleistocene, *Earth Planet. Sci. Lett.*, *65*, 233–244, 1983.

Shackleton, N. J., M. A. Hall, and A. Boersma, Oxygen and carbon isotope data from Leg 74 foraminifers, *Initial Rep. Deep Sea Drill. Proj.*, *74*, 599–612, 1984.

Stein, R., Zur neogenen Klimaentwicklung in Nordwest-Afrika und Palaeo-Ozeanographie im Nordost-Atlantick: Ergebnisse von DSDP-sites 141, 266, 297, und 544B, doctoral thesis, Nr. 4, 210 s, Berichte-Reports, Geol.-Palaeontol. Inst. Univ. Kiel, Kiel, Germany, 1984.

Stott, L. D., J. P. Kennett, N. J. Shackleton, and R. M. Corfield, The evolution of Antarctic surface water during the Paleogene: Inferences of the stable isotope composition of planktonic foraminifers on Leg 113, *Proc. Ocean Drill. Program Sci. Results*, *113*, 849–863, 1990.

Thomas, E., et al., Upper Cretaceous–Paleogene stratigraphy of sites 689 and 690, Maud Rise (Antarctica), *Proc. Ocean Drill. Program Sci. Results*, *113*, 901–914, 1990.

Tucholke, B. E., and G. S. Mountain, Seismic stratigraphy, lithostratigraphy, and paleosedimentation patterns in the North American Basin; in *Deep Drilling Results in the Atlantic Ocean: Continental Margins and Paleoenvironments, Maurice Ewing Ser.*, vol. 3, edited by M. Talwani, W.

Hay, and W. B. F. Ryan, pp. 58–86, AGU, Washington, D. C., 1979.

Tucholke, B. E., and G. S. Mountain, Tertiary paleoceanography of the western North Atlantic Ocean, in *The Western North Atlantic Region, Decade of North American Geology*, vol. M, edited by P. R. Vogt and B. E. Tucholke, pp. 631–650, Geological Society of America, Denver, Colo., 1986.

Tucholke, B. E., C. D. Hollister, F. M. Weaver, and W. R. Vennum, Continental rise and abyssal plain sedimentation in the southeast Pacific basin, Leg 35 Deep Sea Drilling Project, *Initial Rep. Deep Sea Drill. Proj.*, *35*, 279–294, 1976.

van Andel, T. H., Mesozoic/Cenozoic calcite compensation depth and the global distribution of calcareous sediments, *Earth Planet. Sci. Lett.*, *26*, 187–194, 1975.

Vincent, E., J. S. Killingley, and W. H. Berger, The Magnetic Epoch—6 carbon shift: A change in the ocean's $^{13}C/^{12}C$ ratio 6.2 million years ago, *Mar. Micropaleontol.*, *5*, 185–203, 1980.

Vogt, P. R., The Faeroe-Iceland-Greenland Aseismic Ridge and the Western Boundary Undercurrent, *Nature*, *239*, 79–81, 1972.

Woodruff, F., and S. R. Chambers, Mid-Miocene benthic foraminiferal oxygen and carbon isotopes and stratigraphy, Southern Ocean ODP Site 744, *Proc. Ocean Drill. Program Sci. Results*, *115*, 935–940, 1991.

Woodruff, F., and S. M. Savin, Miocene deepwater oceanography, *Paleoceanography*, *4*, 87–140, 1989.

Woodruff, F., S. M. Savin, and L. Abel, Miocene Indian Ocean benthic foraminiferal oxygen and carbon isotopes: ODP Site 709, *Proc. Ocean Drill. Program Sci. Results*, *115*, 519–528, 1990.

Wright, J. D., and K. G. Miller, Miocene stable isotope stratigraphy, Site 747, Kerguelen Plateau, *Proc. Ocean Drill. Program Sci. Results*, *120*, 855–866, 1992.

Wright, J. D., K. G. Miller, and R. G. Fairbanks, Evolution of deep-water circulation: Evidence from the late Miocene Southern Ocean, *Paleoceanography*, *6*, 275–290, 1991.

Wright, J. D., K. G. Miller, and R. G. Fairbanks, Miocene stable isotopes: Implications for deepwater circulation and climate, *Paleoceanography*, *7*, 357–389, 1992.

Zachos, J. C., W. A. Berggren, M.-P. Aubrey, and A. Mackensen, Isotope and trace element geochemistry of Eocene and Oligocene foraminifers from Site 748, Kerguelen Plateau, *Proc. Ocean Drill. Program Sci. Results*, *120*, 839–854, 1992.

Zachos, J. C., L. D. Stott, and K. C. Lohmann, Evolution of early Cenozoic marine temperatures, *Paleoceanography*, in press, 1993.

(Received August 18, 1992;
accepted January 5, 1993.)